POLITECNICO DI TORINO

Master's degree in mechanical engineering

Academic year 2023-2024

Master of Science Thesis

MODELLING AND ENHANCED STABILITY OF A STEER BY WIRE BICYCLE

Supervisors:

Stefano Pastorelli – Politecnico di Torino

Florian Klinger – TU Wien

Manfred Plöchl – TU Wien

Author:

Luca Valenzano

April 2024

TECHNISCHE
UNIVERSITÄT
WIEN
Vienna University of Technology

This Master Thesis has been carried out inside the Technical Dynamics and Vehicle Dynamics department of the Technische Universität Wien under the supervision of the Senior Lecturer Florian Klinger and Professor Manfred Plöchl.

Abstract

In this Master Thesis an innovative approach to bicycle design by introducing a steer-by-wire system is studied, where the traditional mechanical link between the handlebar and fork is replaced by servomotors, sensors, and a controller. The main goals of this research are the following. To begin with, a detailed model of the bicycle and the steer-by-wire system was set up in Simpack, a multibody system simulation software. In this phase, stability analyses are performed, and the need for a control strategy to resolve instabilities at lower forward speeds is highlighted. A linear, discrete time controller was developed in MATLAB-Simulink, and a co-simulation environment was set up between the two softwares to test the controller in conjunction with the bicycle model. Based thereon, different setups of the control parameters were analysed to evaluate the potential of steer-by-wire systems as stability-enhancing mechanisms for straight ahead motion under the constraint of the maximum torque output of the system's actuators. Finally, the interaction of the controller with steering inputs from the virtual driver during cornering and other common cycle manoeuvres was analysed. This research aims to advance the understanding of bicycle control mechanisms and contribute to the development of safer cycling technologies.

Index

Table of figures

1. INTRODUCTION

Riding a bicycle is a skill that many individuals acquire during childhood, relying on specific reflexes to maintain balance and approach desired trajectories. However, such reflexes are not only singular for each specific rider, but could also diminish with age, leading to increased vulnerability, particularly among older or inexpert populations. Indeed, these individuals comprise a significant portion of those injured in road traffic accidents involving bicycles. Recognizing the importance of addressing this issue, research has been conducted on innovative technologies aimed at enhancing bicycle safety and rider assistance.

The challenge of vehicle loss of control, particularly prevalent in Powered Two-Wheelers (PTW), derives from the intrinsic instability of these ones, especially at low speeds. This instability manifests through three primary modes in motorcycle dynamics: capsize, wobble, and weave. Moreover, longitudinal acceleration, especially during braking, poses an additional stability concern. Theoretical proposals for motorcycle handling improvements have been made, although including the elimination of counter-steering behaviour and the introduction of lane-keeping assistance, experimental investigations are limited.

Advancements in control technologies have significantly influenced vehicle dynamics, particularly through the adoption of technologies called "by-wire" in the automotive industry. These methods include various systems in which electronic sensors and actuators replace traditional mechanical components. The control of these actuators is entrusted to software running on a controller, enabling functionalities beyond the capabilities of conventional mechanical-human systems. steer-by-wire technology holds promise for revolutionizing the dynamics of single-track vehicles like motorcycles, scooters, and in our case, bicycles. Existing literature acknowledges the potential benefits of steer-by-wire systems in enhancing vehicle handling and explores the impact of active steer-torque control on the lateral stability of a bicycle, demonstrating in some cases reduced rider effort and increased stability at low speeds. Empirical evaluations on single-track vehicles remain scarce now, this is why this is still considered as an open topic.

The focus will be set on the virtual modelling and experimental validation of an innovative approach to bicycle design, a steer-by-wire system. Additionally, this thesis explores how a steering assistance system can help riders, especially those with weaker reflexes or age-related limitations. The goals will settle on the development of a first model of the vehicle and then the control strategy simulations will take place to assess the feasibility of the stability enhancing properties of the system, especially at lower forward speeds; here different setups have been tested to analyse the impact on the performance. In the end the interaction between the system and a handlebar controller able to simulate steering inputs from the driver have been considered.

1.1 WORKFLOW

A methodological timeline showing the work conducted has been provided below.

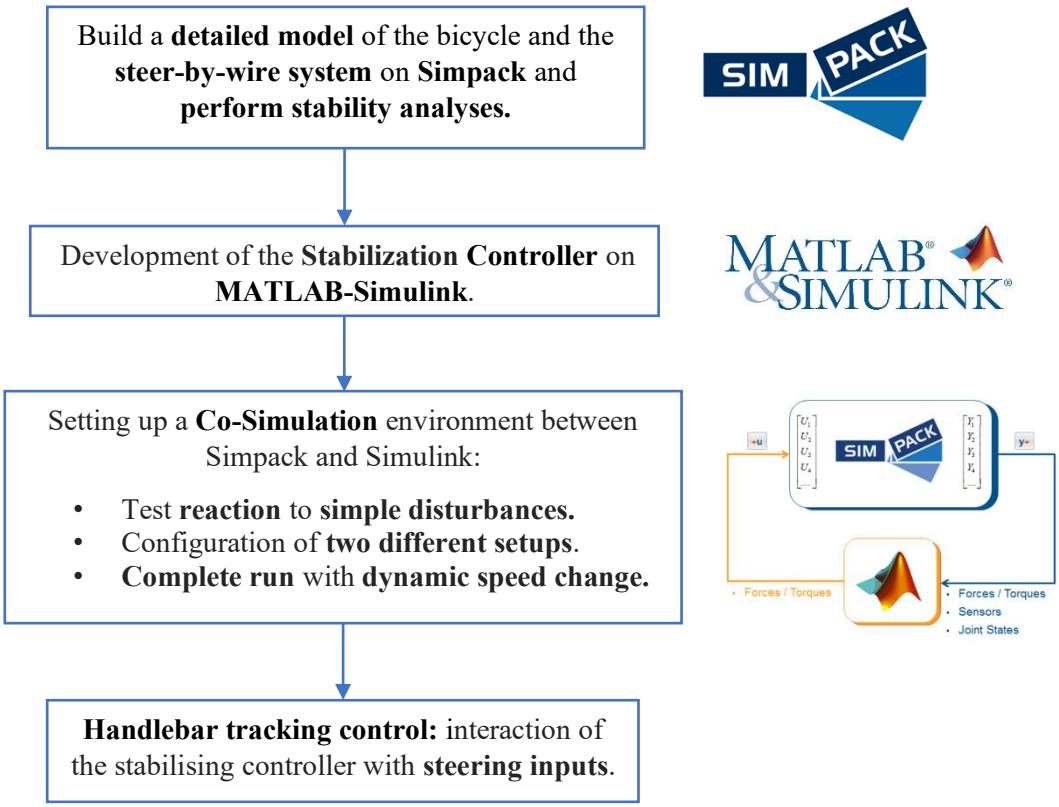

2. RESEARCH AND PREVIOUS STUDIES

Before moving forward, it is first necessary to start from the past research and focus on what has already been done regarding single track vehicle dynamics and stability to fully understand the possibilities available to achieve our goal. Following the evolution of the knowledge on this topic some systems have already been presented as stability-improving.

- A first analysis on two wheels dynamic and behaviour have been carried out by Robin S. Sharp (Sharp R. S., 2008), where it is discussed the analysis of bicycle dynamics, particularly focusing on the stability and auto stabilisation of bicycles, based on the re-examination of the Whipple and Carvallo model. The eigenvalues of the benchmark bicycle's characteristic equation are computed across different speeds (*Figure 1*). At 0.2 m/s, two divergent modes with associated ratios of steer to roll are observed and as speed increases, the eigenvalues converge and form an oscillatory weave mode, stabilizing at 4.29 m/s. The benchmark bicycle exhibits self-stabilisation in the speed range 4.3 – 6 m/s, with a zero-eigenvalue marking the capsize mode at 6 m/s.

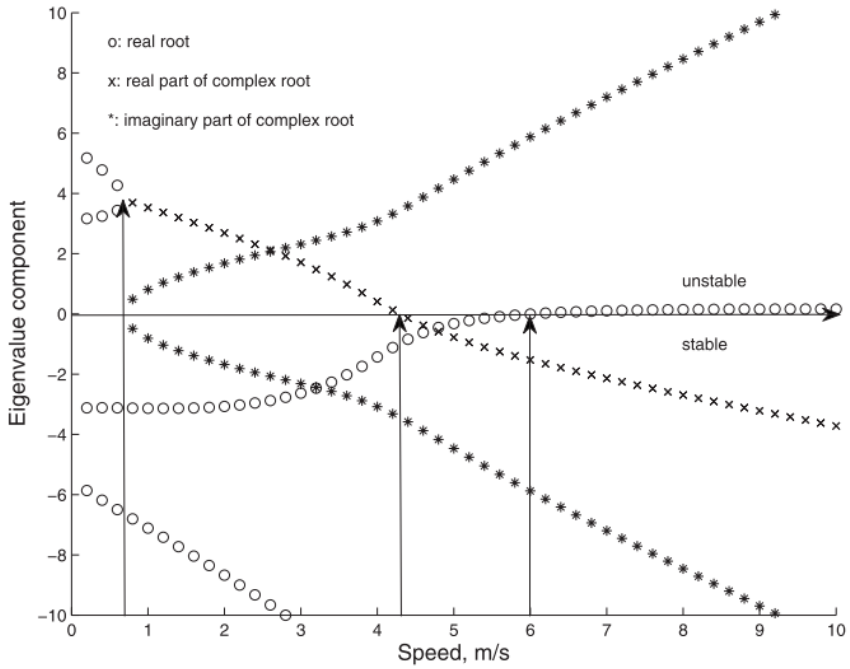

Figure 1: Eigenvalues of the benchmark bicycle over 0.2–10 m/s speed range.

Here a linear optimal control preview is used in order to succeed in the goal of the steering control of the bicycle. It is noticeable how skilled riders have more significant control influences, such as larger steering torques, than what is implicit in bicycle mechanics. Once riding skill is developed, riders become relatively insensitive to variations in bicycle design, as they can easily countermand the effects of bicycle mechanics. The implementation of the preview control demonstrates how riders can use knowledge of the forward path and prioritize accuracy and control power to follow a desired path, similarly to a feedforward strategy. Furthermore, the evaluation of systems with steer-torque control and combined steer and rider-lean torques reveals that rider control is less important than steer-torque control when both are available.

- Shwab shows (A. L. Schwab, 2013) a comprehensive examination of the steer-by-wire bicycle's design and performance. The aim is to validate the feasibility and efficacy of an innovative approach. Preliminary rider tests have been done and some promising results have been displayed, with perceived behaviour getting closer with that of a traditional mechanical connection, particularly at steering frequencies below 3 Hz. A three degree of freedom Whipple/Carvallo bicycle model (Whipple, 1899) is taken into consideration (*Figure 2*); it is formed by four rigid bodies: a rear frame including the rider as a rigid mass with no hands on the handlebars, a front frame which consists of the handlebar and fork assembly a rear wheel and a front wheel. Then the handlebar is separated from the front fork, like in this case.

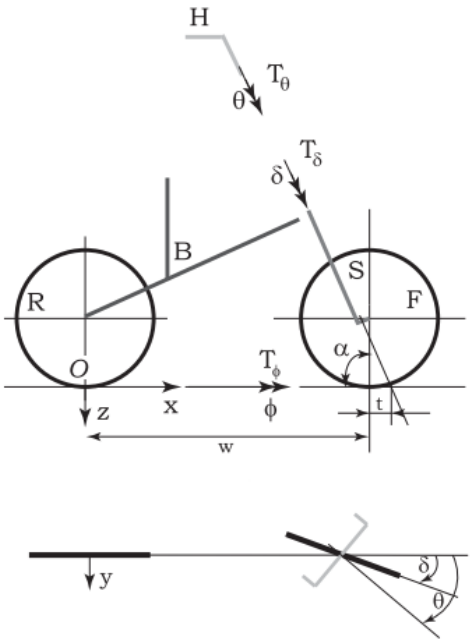

Figure 2: Steer by wire model and linear equation of motion.

There are some control elements as well, implemented to increment the system stability. First, a Proportional-Differential (PD) tracking control, with its relative gain values, on the handlebar allows to get the handlebar and the steering angle closer so that their minimized difference makes the bike more similar to an ordinary one. Then, the focus shifts on addressing the inherent instability in lateral motions at low speeds; to stabilize these motions, a steer-torque control system is integrated, alongside the already existing one. Specifically, a steer-into-the-fall controller is adopted (*Figure 3*); this controller utilizes the roll rate of the rear frame as an input and outputs steer-torque. The integration of this controller aims to enhance the low-speed stability of the bicycle, providing a robust solution to mitigate lateral motions and improve overall control during critical manoeuvres at reduced speeds.

A complete idea of the relative block diagram is shown below, as well as the eigenvalue graph (*Figure 4*) representing the changing in the speed stable range, which shows the lowest weave speed going from 4.3 m/s to 1 m/s.

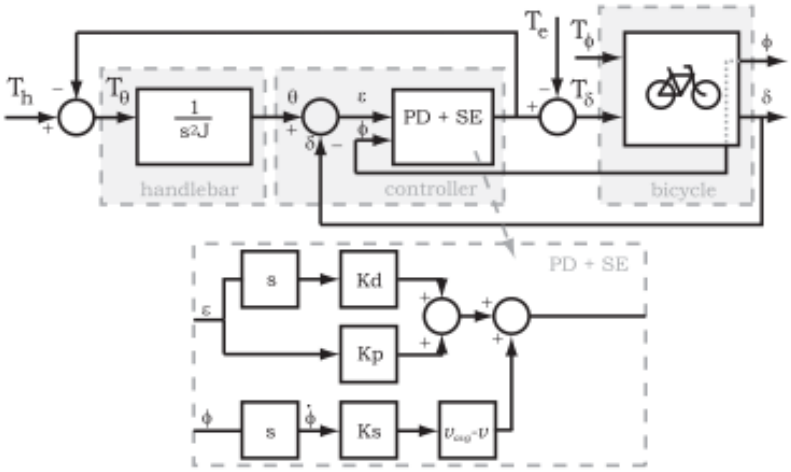

Figure 3: Block diagram of the steer-by-wire bicycle model.

The results highlight a highly satisfactory behaviour, in which the rider is unable to discern a notable difference in handling compared to a bicycle with a conventional rigid steering connection; only a close observation makes a minor phase lag between the handlebar and the steering assembly noticeable, which did not significantly impact the perceived handling. This study marks a significant step towards advancing the understanding of bicycle dynamics and opens doors to the potential integration of steer-by-wire technology as part of the bicycle reality.

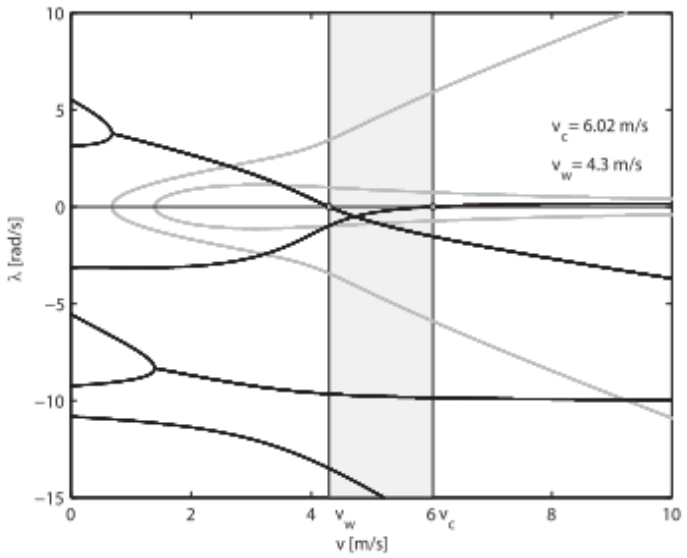

a)

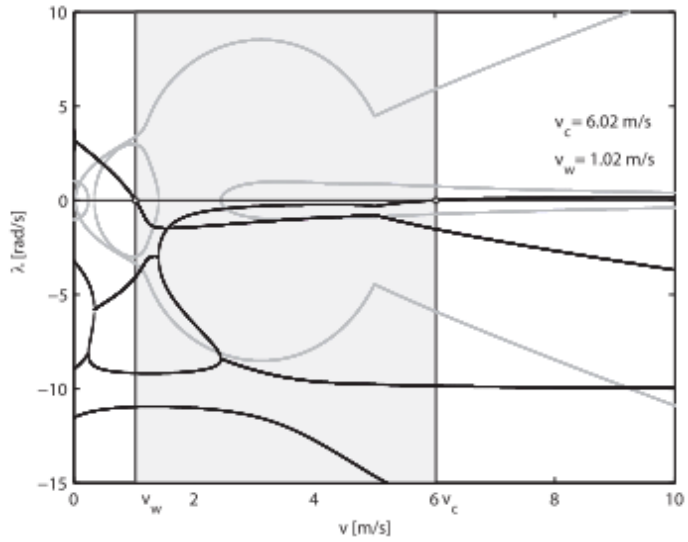

b)

Figure 4: Eigenvalues λ from the linearized stability analysis for a) the original steer-by-wire benchmark bicycle model in comparison to b) the eigenvalues for the same model with added lateral stability control.

- A follow up of the previous study (G. Dialynas, 2018) dives into the importance of haptic feedback on steering behaviour for a given set of control tasks and on how this can lead to the development of new design criteria for safer bicycles. The system design is the extension of the one showed in *Figure 2* with the introduction of an additional degree of freedom from the separation of the handlebar from the front fork and it includes a double PD controller (one for the handlebar and one for the fork), with rider applied steering torque, feedback steering torque and steering from the handlebar and fork applied torque and angle (*Figure* 5).

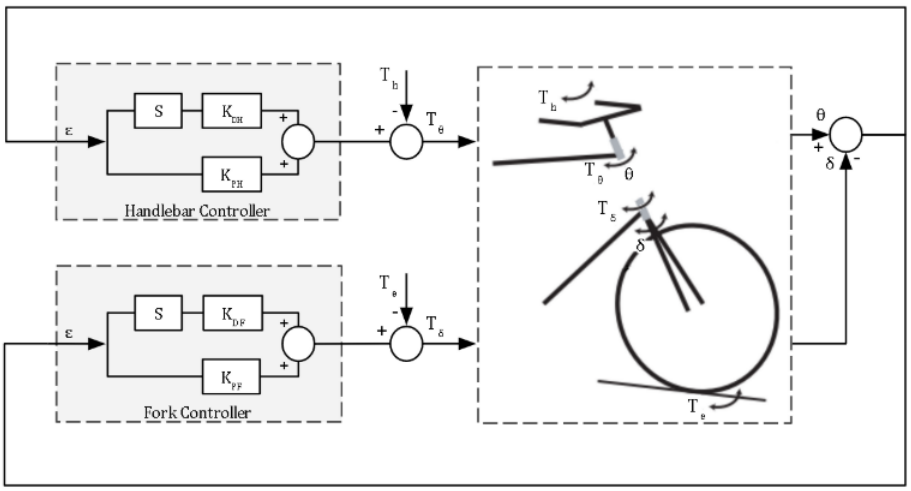

Figure 5: Block diagram of the steer-by-wire bicycle model.

After some tests it is important to mark that the bicycle handlebars using the steer-by-wire technology have greater flexibility, achieving also a larger steering angle with the same amount of steering torque input. The variance in handlebar steering stiffness may suggest an increased effort required by the rider to steer, but it does not have any impact on the overall stability of the bicycle. The realization of the physical model follows in *Figure 6*.

Figure 6: Steer by wire bicycle prototype and system close up.

After tests composed of a set of slalom manoeuvres in the stable and unstable bicycle speed region, it was noticed that even without any training, all the riders were able to control the steer by wire bicycle as if it had a classical mechanical connection.

- A more modern study performed in 2022 (Georgios Dialynas, 2022) and based on the previous one, launches a new approach for the steer by wire bicycle reconfiguring parameters, developing a new rider model which can consider the steering torque feedback. Moreover, here also the human

capabilities to adapt to some feedback lag and the effect of handlebar torque and position feedback is taken into consideration. The experimental trials involved testing four different speeds (2.6, 3.7, 4.5, and 5.6 m/s) to cover stable and unstable forward speed ranges; furthermore, lateral perturbations from impulsive forces are included. Focusing on haptic steering torque feedback, the experiment involved rider models with feedback loops for visual/vestibular motion, steering torque, and steering angle while considering sensory delays. Marginal effects of haptic steering torque feedback on steering actions and bicycle motion have been found. The best model performance was observed with haptics on and a feedback configuration which was including the Torque. The study also addressed sensory delays: comparing zero delays (ZD) and sensory drop (SDROP) models, revealing almost identical responses and it also highlighted the increased importance of heading control at higher speeds. The SDROP model's sensory delay uses an internal forward model, while the SD one shows that this sensory delay implementation causes mismatch between results and experimental data if a feedforward compensation is left aside. It is also possible to find a way to control the bicycle at each speed through a fitted rider model.

- Another similar yet with some structural difference solution is an active steering assistant (AciSA), which has been taken into consideration and studied a few years ago (S. Lovato, 2022). Even if the system does not refer to a Steer by wire technology, it is worth noting that the technology used here is a valid alternative for a similar purpose; here the mechanical connection between handlebar and the fork is maintained (*Figure 7*), differently from the SBW, in view of avoiding raising safety concerns in case of system failure, preserving the handling capabilities of the vehicle, yet keeping the stabilisation features; a steering torque between the vehicle chassis and the front assembly is still applied. The characteristic of this system also takes advantage of another technology which is inspired by: the Gyroscopic Stabilizers. Is important to mark that pure gyroscopic systems

are heavier, more expensive, and request more energy, while here only the perk of stabilisation in wide range of operating speed, especially at very low ones, is accounted.

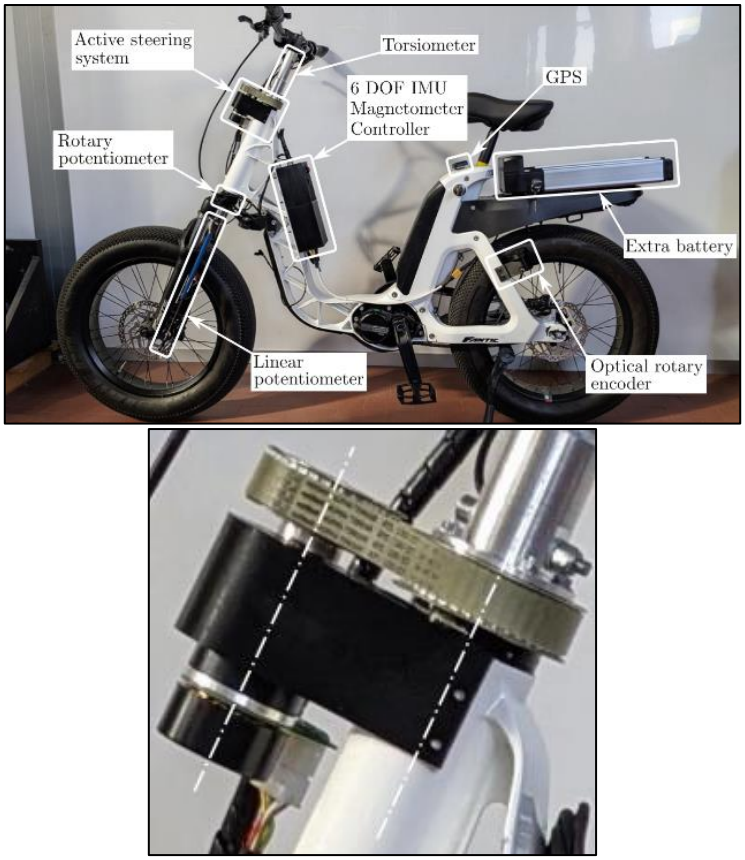

Figure 7: Active steering assistant bicycle.

The e-bike used is equipped with 3 subsystems, one for the active steering, one for the rider steering torque measure and one for the vehicle motion measure: the first is a brushless DC motor coupled with a planetary gearhead and a belt drive transmission, the second has a torsiometer integrated with the steering shaft, while the third integrates many sensors. The experimental tests to validate system reliability, data acquisition, and instrument performance revealed consistency of the system with reference to the applied rider torque and shows the capability of the on-board instrumentation.

3. SYSTEM DESIGN

The benchmark bicycle taken as initial starting point is a restatement of the Whipple/Carvallo model (*Figure 2*) and it can be summarized as a rider attached rigidly on the main frame with hands on the handlebar, with a front frame connected via a perfect revolute joint inclined to the vertical. This model of the bicycle tends to present low-to-no stabilisation capability at lower forward speeds and the aim of the controller is to deal with this deficiency. This is why the traditional vehicle will be modified decoupling the mechanical connection on the fork between its lower part and the handlebar, applying subsequently a correction in a Torque form managed by a controller. The lateral and steering stability of the whole would be improved.

3.1 A STARTING POINT: BENCHMARK BYCICLE AND HUMAN MODEL

Focusing on the benchmark bicycle implemented on MATLAB, it is represented by its linearized equation of motion containing the state vectors $\boldsymbol{q}$, $\dot{\boldsymbol{q}}$ and $\ddot{\boldsymbol{q}}$, describing the four degrees of freedom of this case:

Equation of motion:

$$\boldsymbol{M}\cdot\ddot{\boldsymbol{q}}+(\boldsymbol{C_0}+\boldsymbol{u}\cdot\boldsymbol{C_u})\cdot\dot{\boldsymbol{q}}+\boldsymbol{K_0}\cdot\boldsymbol{q}=Q_{ext}=Q_{tyre}+Q_{rider}$$

State vector:

$$\boldsymbol{x}=[\boldsymbol{q},\dot{\boldsymbol{q}}]^T$$

Where:

$$\boldsymbol{q}=[\varphi,\delta]$$

$$\dot{\boldsymbol{q}}=[v_y,r,\ \dot{\varphi},\ \dot{\delta}]$$

$$\ddot{\boldsymbol{q}}=[\dot{v_y},\ \dot{r},\ \ddot{\varphi},\ddot{\delta}]$$

With:

- φ = roll angle.
- δ = steering angle.
- v_y = lateral velocity.
- $r = \dot{\psi}$ = yaw angle velocity.
- $\dot{\varphi}$ = roll velocity.
- $\dot{\delta}$ = steering velocity.

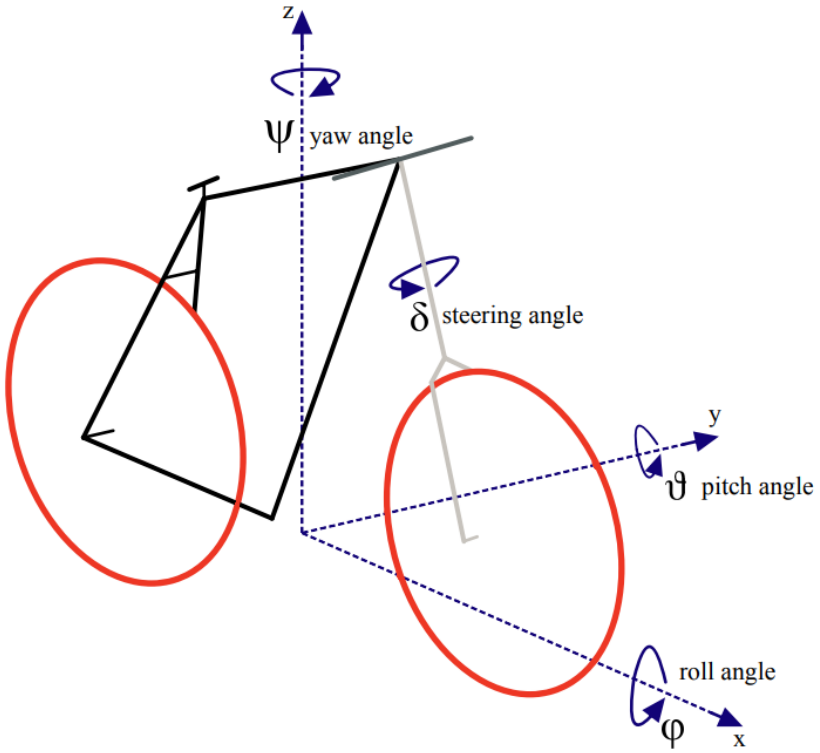

Figure 8: The benchmark bicycle model and his states around the reference system.

Specifying what is included in the Equation of motion, $\boldsymbol{M}$ is the mass matrix, $\boldsymbol{C_0}$ and $\boldsymbol{C_u}$ are the damping matrices with the first one constant and second one depending on the forward velocity u, $\boldsymbol{K_0}$ as the stiffness matrix. In the end the forcing term $Q_{ext} = Q_{tyre} + Q_{rider}$ with the torque coming from the tyres Q_{tyre} and the torque coming from the rider Q_{rider}.

Each of the five main bodies composing the vehicle, the frame, the fork, the handlebar and the two wheels, has its specific mass, dimension, centre of gravity (CoG) and inertia tensor set at its initial values. The starting model also had a set of

parameters defining the physical properties of the linear Tyre Model (Pacejka, 2012) which characterizes the behaviour of the tyres in contact with the ground.

The human body present on the bicycle refers to the study lead by Ernest P. Hanavan Jr (Ernest P. Hanavan. Jr., October, 1964), and it is based on an experimentally determined distribution of mass and the anthropometric data of the individual person, so that its mathematical model can help predicting its inertial properties in any fixed position. The human body is represented by a set of sixteen rigid bodies of simple geometric shape and uniform density: head, upper torso, lower torso, lower torso 2, right hand, left hand, right upper arm, left upper arm, right forearm, left forearm, right upper leg, left upper leg, right lower leg, left lower leg, right foot, left foot.

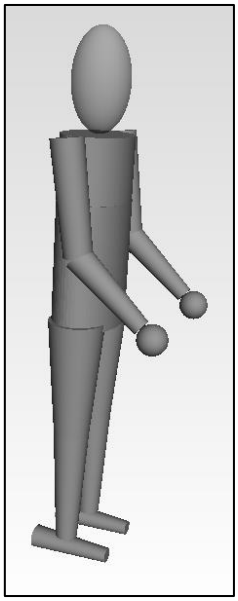

Figure 9: The Hanavan human body model.

The overall mass can be adjusted to accommodate the specific requirements of tests, with an initial configuration fixed at 73.4 kilograms. It is possible to tailor the geometry of the joints holding the role to connect the sixteen bodies of the human model. By changing the x-y-z positions and the rotation around these axes manually, it is possible to adapt the 0-degree of freedom joints to the bicycle's elements, placing the rider in the pre-determined position of interest. A joint of particular concern is the "lower torso 2", denoting the rider's saddle position.

3.2 MULTIBODY SIMULATION - SIMPACK

Multibody simulation (MBS) numerically simulates the behaviour of interconnect rigid or elastic bodies, using kinematic constraints and force elements to model connections and it is particularly useful to evaluate comfort, safety, and performance characteristics. SIMPACK is a software tool primarily used for this in engineering applications. Key elements of it include its ability to model complex mechanical systems, simulate dynamic interactions, and provide insights into the structural and kinematic behaviour of these systems; it is commonly used for studying and optimizing the performance of vehicles, machinery, and other mechanical systems.

To have an initial general clue of the software, it is useful to refer to the main page in which all the most important features are displayed (*Figure 10*):

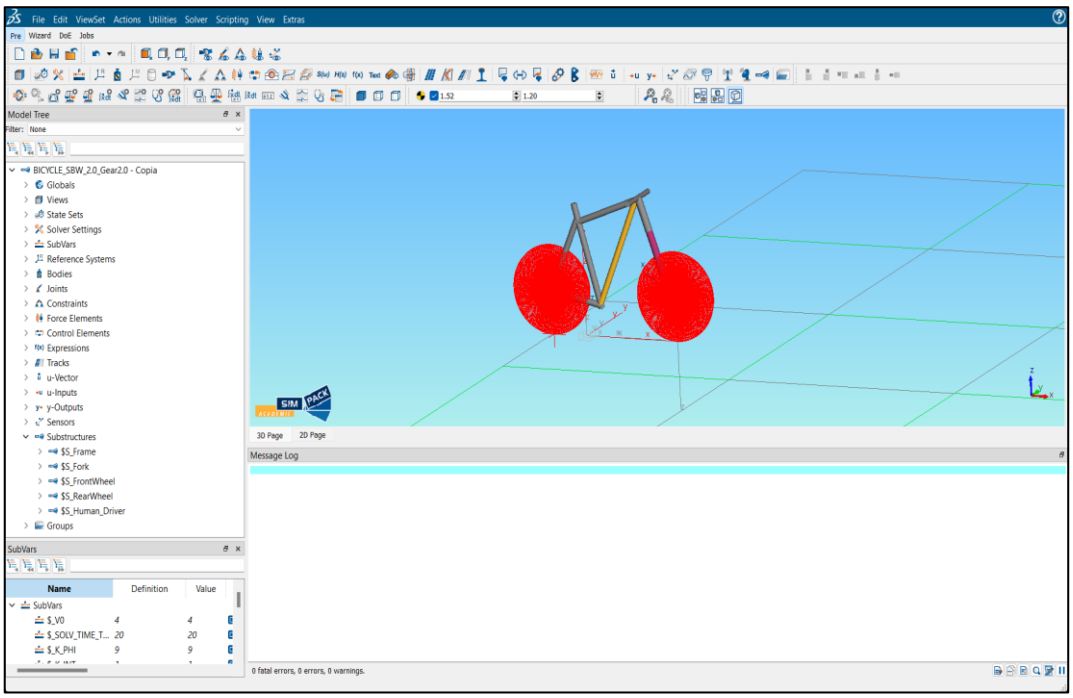

Figure 10: Front interface view of SIMPACK.

On top of the main interface page the Menu bar (containing items such as File, Edit, etc.), beneath the ViewSets in which it is possible to switch between the ViewSets (Pre, Wizards, DoE, Jobs) and the toolbar below, containing all the main features present on Simpack. Then on the left side there is the Model Tree where the models

opened by the user, as well as their modelling element categories and the individual element types, are displayed. On his right, the 3D page providing a 3D interactive graphical representation of the model in space, with the global coordinate system shown at the bottom right-hand corner. This view can be also switched with the 2D page, where an alternative model view in a block diagram fashion is shown, with blocks, symbols, and connection lines composing the main model topology. Beneath, the Message Log provides information generated by different processes on the running model, showing warnings and errors. Then last, on the low left corner, the SubVar ViewSet element shows the sub-variables used in the Model Tree elements, having here the possibility of being modified.

In this case the primary goal is to set up an initial model, able to recreate the behaviour of a real conventional bicycle and then add the steer by wire system to perform some tests afterwards, increasing complexity in the process.

3.3 SET UP OF THE FIRST BICYCLE MODEL AND STABILITY ANALYSES

The first version of the vehicle has been set up following the initial idea of a scooter, implemented with all the inertia/geometric values of the initial bicycle. In *Table 1*: Masses and geometry of the main com ponents of the system it is possible to see all the main parameters such as masses, geometry centre of gravities and inertia properties. It is important to keep these into account since both the adding of the rider and the steer by wire systems will have a direct impact on the equilibrium of the system.

COMPONENT	PARAMETER	VALUE
Main frame		
	Mass	9.98 kg
	Centre of gravity (CoG) (x_{mf}, y_{mf}, z_{mf})	(0.2397, 0, -0.6006) m
	Inertia tensor with respect the CoG $\begin{bmatrix} I_{xx} & I_{xy} & I_{xz} \\ I_{yx} & I_{yy} & I_{yz} \\ I_{zx} & I_{zy} & I_{zz} \end{bmatrix}$	$\begin{bmatrix} 0.6868 & 0 & -0.0004 \\ 0 & 1.3745 & 0 \\ -0.0004 & 0 & 0.7612 \end{bmatrix}$ kgm^2
Fork		
	Mass	2.4 kg
	Centre of gravity (CoG) (e_f, y_f, d_f)	(0, 0, -0.3) m
	Inertia tensor with respect the CoG $\begin{bmatrix} I_{ex} & I_{ey} & I_{ed} \\ I_{ye} & I_{yy} & I_{yd} \\ I_{de} & I_{dy} & I_{dd} \end{bmatrix}$	$\begin{bmatrix} 0.6868 & 0 & -0.0004 \\ 0 & 1.3745 & 0 \\ -0.0004 & 0 & 0.7612 \end{bmatrix}$ kgm^2
Handlebar		
	Mass	1.63 kg
	Centre of gravity (CoG) (e_f, y_f, d_f)	(-0.07055, 0, -0.7231) m
	Inertia tensor with respect the CoG $\begin{bmatrix} I_{ex} & I_{ey} & I_{ed} \\ I_{ye} & I_{yy} & I_{yd} \\ I_{de} & I_{dy} & I_{dd} \end{bmatrix}$	$\begin{bmatrix} 0.056777 & 0 & 0.00104 \\ 0 & 0.03517 & 0 \\ 0.00104 & 0 & 0.05656 \end{bmatrix}$

Rear wheel		
	Mass	2.35 kg
	Radius	0.3355 kg
	Inertia tensor with respect the CoG $\begin{bmatrix} I_{xx} & I_{xy} & I_{xz} \\ I_{yx} & I_{yy} & I_{yz} \\ I_{zx} & I_{zy} & I_{zz} \end{bmatrix}$	$\begin{bmatrix} 0.06482 & 0 & 0 \\ 0 & 0.1296 & 0 \\ 0 & 0 & 0.06482 \end{bmatrix}$ kgm^2
Front wheel		
	Mass	1.95 kg
	Radius	0.3355 kg
	Inertia tensor with respect the CoG $\begin{bmatrix} I_{xx} & I_{xy} & I_{xz} \\ I_{yx} & I_{yy} & I_{yz} \\ I_{zx} & I_{zy} & I_{zz} \end{bmatrix}$	$\begin{bmatrix} 0.06332 & 0 & 0 \\ 0 & 0.1266 & 0 \\ 0 & 0 & 0.06332 \end{bmatrix}$ kgm^2
Rider		73.4 kg
Total mass of the bicycle		18.3 kg
Total mass of the bicycle + rider		91.7 kg
Wheels distance		1.095 m
Steering rake angle		71 °
Trail		0.069 m
Fork offset		0.04 m
Handlebar width		0.405 m
Wheels radius		0.3355 m

Table 1: Masses and geometry of the main com ponents of the system.

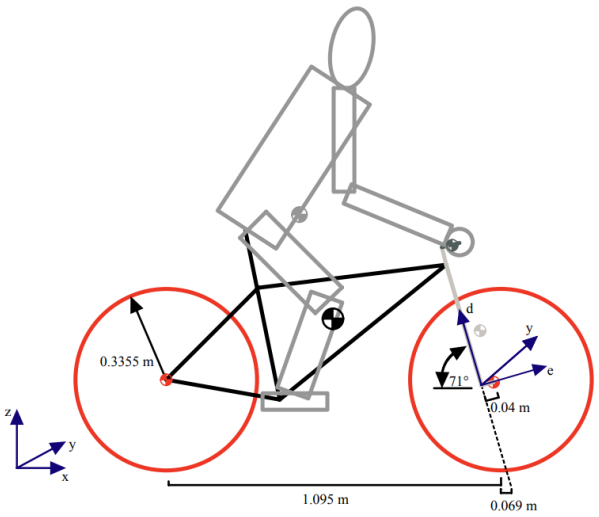

Figure 11: Sketch of the bicycle with system of reference and main geometric features.

Next, the tyre model has been included, specifying characteristics linked to tyre slipping with respect to the ground and stiffness. These parameters refer to the studies which can be found in the "Tire and Vehicle Dynamics" book (Pacejka, 2012), a comprehensive resource on the dynamics of tires and vehicles, particularly focusing on the modelling and analysis of tire behaviour, which is also devoted to the analysis of the properties of a theoretical tire model through simple physical model and their application in vehicle dynamics simulations and control systems.

PARAMETER	SYMBOL	VALUE
Front wheel		
Slip angle stiffness	$c_{F\alpha 1}$	12.6 N/rad
Camber angle stiffness	$c_{F\Upsilon 1}$	0.86 N/rad
Self-aligning Torque due to slip angle	$c_{M\alpha 1}$	0.0273* $c_{F\alpha 1}$ Nm/rad
Self-aligning Torque due to camber angle	$c_{M\Upsilon 1}$	0.0432* $c_{F\Upsilon 1}$ Nm/rad
Inner length slip angle	$\sigma_{\alpha 1}$	0.06 m
Inner length camber angle	$\sigma_{\Upsilon 1}$	0.06 m
Rear wheel		
Slip angle stiffness	$c_{F\alpha 2}$	10.3 N/rad
Camber angle stiffness	$c_{F\Upsilon 2}$	0.85 N/rad
Self-aligning Torque due to slip angle	$c_{M\alpha 2}$	0.025* $c_{F\alpha 2}$ Nm/rad
Self-aligning Torque due to camber angle	$c_{M\Upsilon 2}$	0.0325* $c_{F\Upsilon 2}$ Nm/rad
Inner length slip angle	$\sigma_{\alpha 2}$	0.06 m
Inner length camber angle	$\sigma_{\Upsilon 2}$	0.06 m

Table 2: Tyre parameters.

The building of the model started from the initial arrangement of the geometry and the creation of the five substructures present in *Table 1* using the features SIMPACK displays: creation of bodies, their geometry, markers, joints/connections, constraints and additional elements as forces/torques or controllers. The purpose behind the use of substructures is the isolation of the categories of the bodies, so that the work involving each of them can be taken separately. Once that the bicycle model was successfully set up, the driver has been incorporated into it (*Figure 12*) and coupled with the saddle point and taking into account to keeping his hands still and steady on the handlebar, making the whole

system ready to be stability-tested in view of a first confrontation with the ideal behaviour.

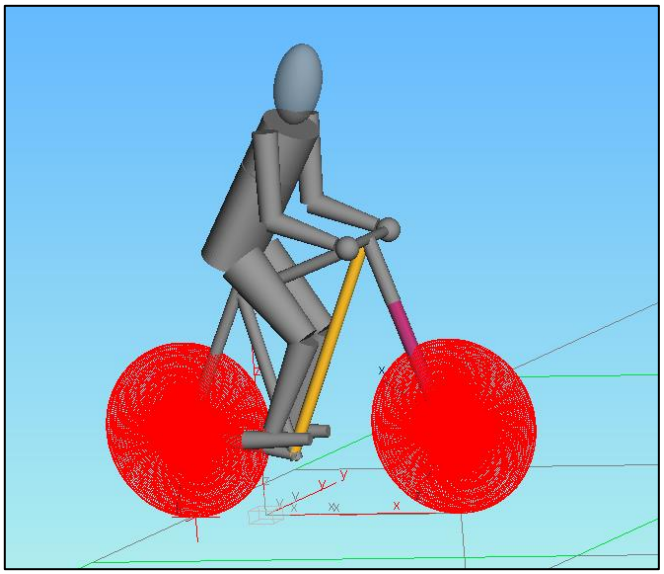

Figure 12: First model of the assembly bicycle and driver.

The process started from selecting a set of thirteen velocities (1.5, 2, 4, 6, 8, 10, 12, 14, 16, 18, 20, 22, 24 m/s) and apply them to a Cruise Controller module on Simpack keeping the speed constant throughout the simulation, then run it and derive the eigenvalues to plot and compare with the ones coming from MATLAB (*Figure 13*).

The graph shows two types of modes, in other words two different behaviour: the weave is an oscillatory lateral motion which causes the vehicle to sway from side to side, presenting instability risks at both low and high speeds, while the capsize is a non-oscillatory motion, which when unstable especially at low speed corresponds to a slowly lean and eventually toppling over. The capsize is then considered stable in all the range of speeds in this case, while the weave mode needs a stabilisation strategy before 9 m/s.

In a system analysis, particularly in control theory, the eigenvalues of a system's dynamics matrix play a crucial role and the positive/negative real part and positive/negative imaginary part of the eigenvalues have a core influence on the behaviour of it. To have a closer look on them:

- Positive real parts of eigenvalues indicate exponential growth in the corresponding mode and in this context, it implies unstable behaviour. For instance, if the bike starts to tilt to one side, a positive real part eigenvalue

would imply that this tilt continues to grow over time, leading to instability and possibly a crash and then representing an uncontrollable and diverging motion, leading the bike to a loss of control.

- Negative real parts of eigenvalues indicate exponential decay in the corresponding mode, so in the two wheels vehicles if the bike tilts to one side due to an external disturbance, the negative real part eigenvalue would indicate that the tilt decreases over time, bringing the bike back to its equilibrium position. It is then a stable and controllable behaviour.
- The imaginary parts both indicate a stable and oscillatory behaviour, so for the system it might manifest as a wobbling or oscillating motion. This could be observed when a rider tries to maintain balance, causing the bike to oscillate around the upright position. The difference between the positive and negative one lays in the phase or direction of the motion, which is opposite.

It is from this evaluation phase that it was noticeable the obvious relation between the velocity and the time the bike was standing: the more the velocity, the sooner the oscillation of the vehicle was starting, provoking the subsequent fall and in an analogue yet opposite way, the tendency in recovering from initial given instabilities got faster as the velocity was rising. This is an aspect that will be explored in depth in the next chapter when the comparison between Open Loop and Closed Loop achieved with the control strategy will be carried out.

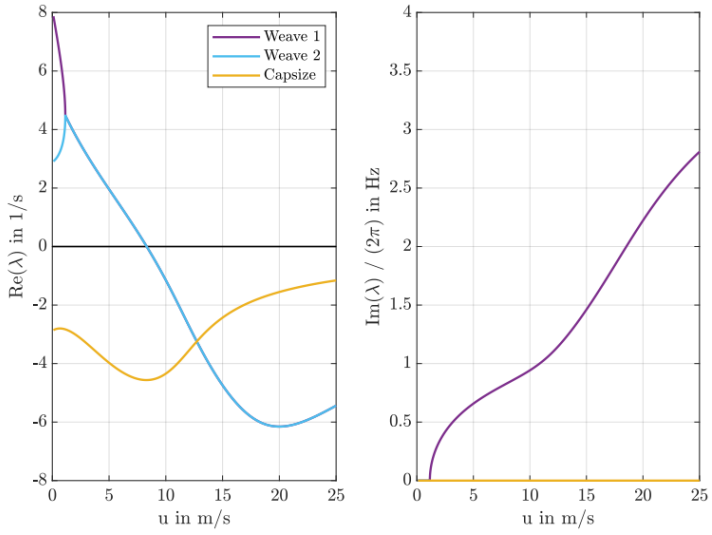

Figure 13: Eigenvalue graph of the ideal behaviour of the bicycle model: Real part of the eigenvalues on the left and Imaginary on the right.

After performing the evaluation, at first time it was clear the lack of correspondence between the SIMPACK and the MATLAB ideal one (*Figure 14*), which almost disappeared after a more accurate estimation of the masses and geometry of the system and the choice of a linear tyre model.

Now that the corrected model is trustworthy and stable, there is a solid basis where to apply the additional system and proceed with the next phases.

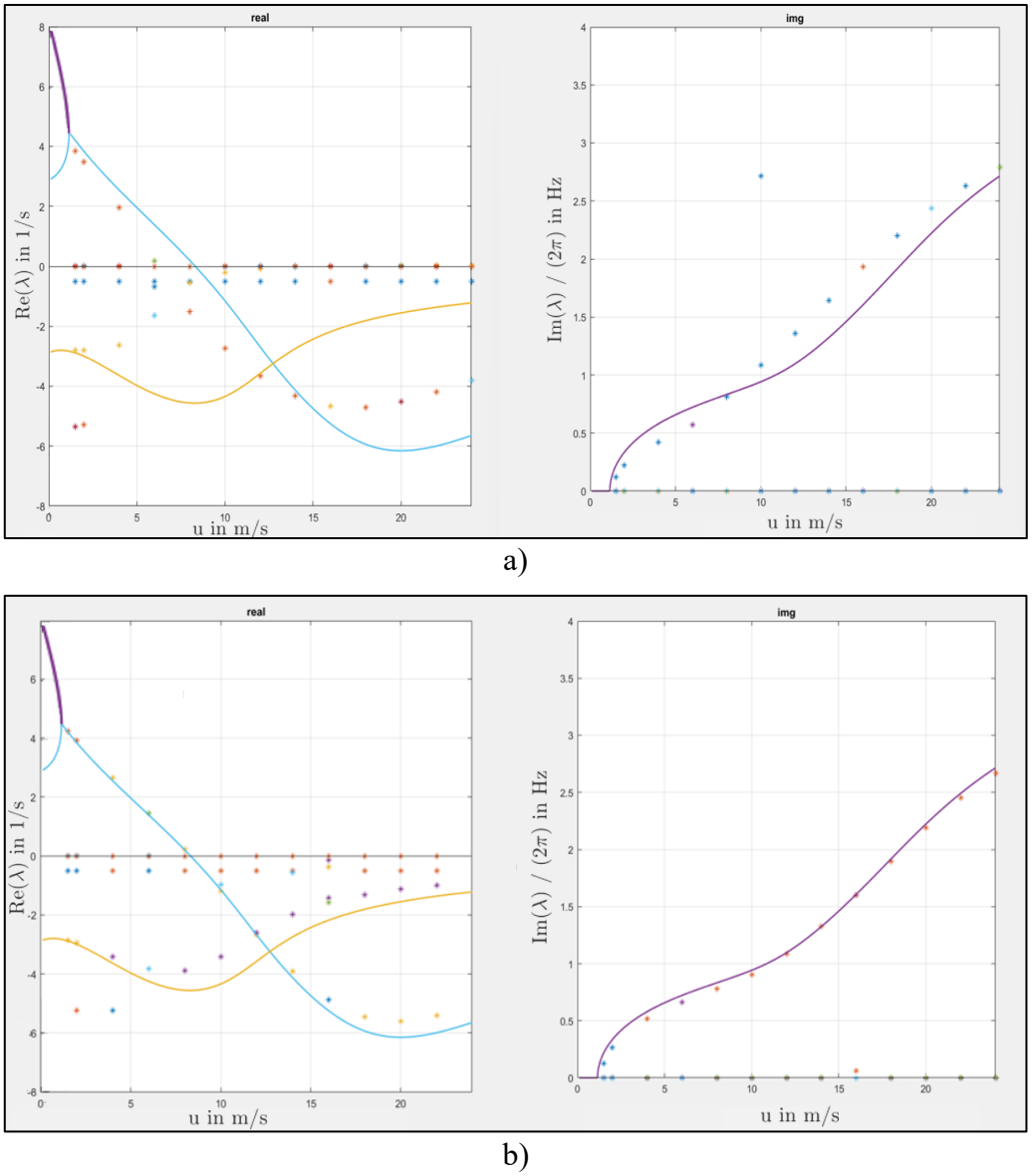

Figure 14: Comparison between eigenvalue graphs before a) and after b) a "fitting". The continuous line represents the MATLAB model while the dots come from the Simpack evaluation.

It is now the role of the steer by wire system to manage to move the range of stability to lower velocities and rearrange the eigenvalues through the control law will be one of the main aspects to achieve it. This will be pursued through the application of a torque feedback on the front fork by a set of motors, encoders, gearboxes, and pulleys presented in the following paragraphs.

3.4 IMPLEMENTATION OF THE STEER BY WIRE SYSTEM

The objective of obtaining a feedback torque capable to compensate the instabilities of the bicycle can now face an application with the design of the steer by wire system. The idea relating the assembling and building of the system started from an initial 3D representation of it, useful to have a first concept which could consider the dimension of the whole (*Figure 15*).

The first main aspect to consider is the disconnection between the upper and the lower part of the fork, which takes place right below the handlebar, while the installation involves an arrangement on the front part of the vehicle, alongside with the frame and in proximity of the top part of the fork itself.

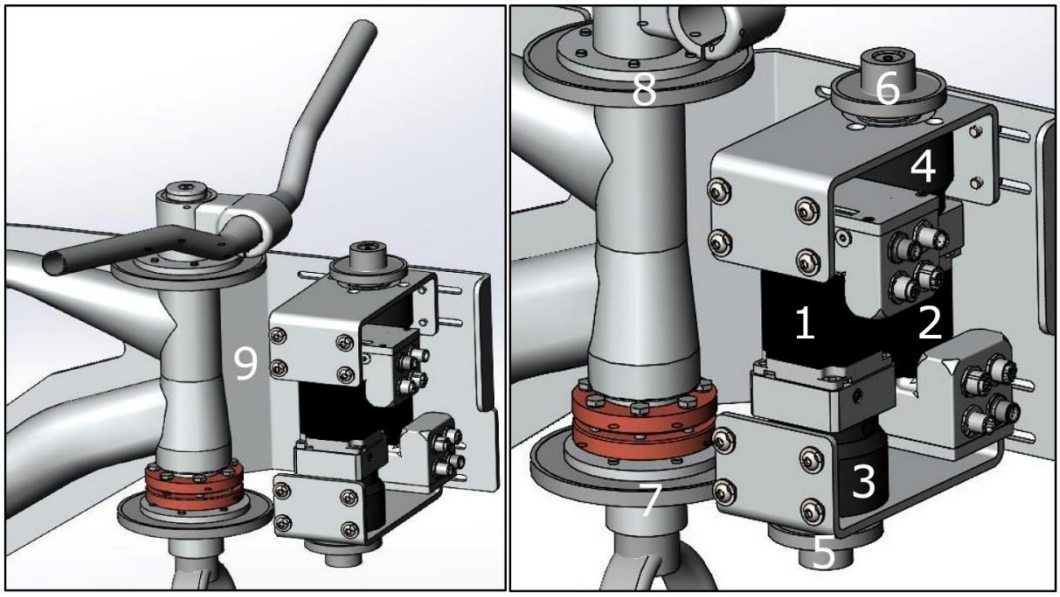

Figure 15: 3D representation of the steer by wire system.

The structure is mainly composed of four types of elements: two electric stepper motor with an integrated controller (1-2), two planetary gearboxes (3-4), two pulleys on the system (5-6) and two on the fork (7-8) and a steel board (9) with plates, screws, and bolts to hold the components together.

COMPONENT		***MASS***
2x Electric Stepped Motor - STEPPER MOTOR WITH INTEGRATED CONTROLLER IP65 – NEMA 23/24		2.6 kg (1.3 kg each one)
	Rotor	0.3 kg
	Stator + Encoder	1 kg
2x Planetary Gearboxes		1.8 kg (0.9 kg each one)
2x Pulleys on the fork		0.4 kg (0.2 kg each one)
2x Pulleys on the SBW system		0.4 kg (0.2 kg each one)
Steel board, plates, and other components		1.5 kg
TOTAL MASS		6.3 kg (+ 0.4 kg on the fork)

Table 3: Steer by wire main components.

The core of the functionality is the possibility to obtain the correction of lateral instabilities while keeping the natural sensation of riding a traditional mechanical linked bicycle, this is possible thanks to the devices implemented (*Table 3*). As it can be seen in the previous picture there are two stacks of elements one next to the other linked using plates and both of them attached to the frame structure by a board: looking at it from the front position, the right one is connected to the upper part of the fork, the one including the handlebar, while the left one refers to the lower part. Each one of these sets include the motor with his encoder, a gearbox, and a pulley, with this last one coupled to the fork through a belt driven system and another pulley strategically positioned on it. The two Electric motors are the pivotal components of the steer by wire, they are prompted from their respective encoder of the signal to generate the right torque to compensate the instabilities detected by the sensors on the bicycle. Subsequently, the connection to the pulleys occurs through a gearbox with a gear ratio of 1:10 for both the upper and the lower part, this will give the inertia of the motor a substantial contribution to the overall inertia of the system; it is through these pulleys that the torque imparted by the motors is transmitted to the fork.

The study which will follow has been divided into three different parts, in order to focus on a subsequently complex environment and dig deeper into the functionality of it. Initially the whole system is being tested without any torque in input so that all the elements will work as idler gears following the fork natural rotation during the instabilities responses and highlighting the only effect of the added mass and inertia of the rotating part. What comes out from this first case is the comparison which can be seen in the following graphs (*Figure 16*): there is, obviously, an influence coming from the weight and inertia of the rotating elements of the steer by wire system elements, on the other hand it doesn't lead the behaviour of the vehicle and the eigenvalue graph being different in a critical way if compared with the one in *Figure 14*.

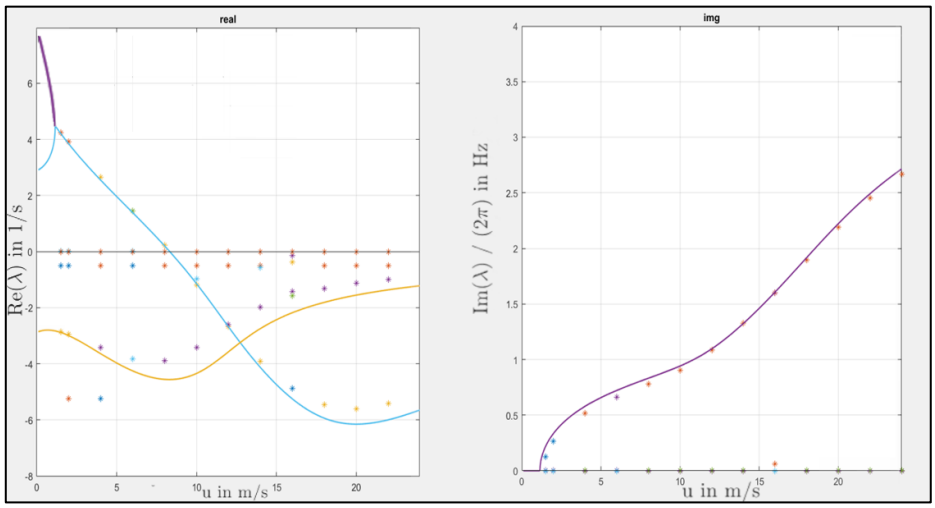

(a)

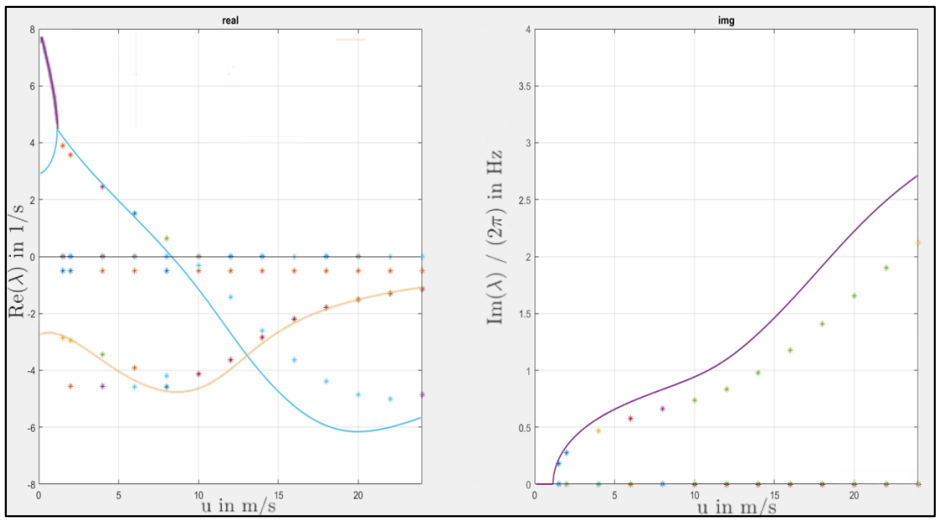

(b)

Figure 16: Comparison between eigenvalues without SBW system (a) and with it installed (b).

What followed had been the application of an additional torque on the half of the system linked to the bottom part of the fork to compensate for the instabilities coming from there working as feedback; this phase has the main goal of the stabilisation. The signal coming from the controller starts the rotor of the motor, letting the torque go through the transmission, being reduced, and transferred to the pulley linked on the steering head. This will make the fork counter-rotate when the vehicle is subjected to disturbances.

Subsequently the whole concept enlarged, and this additional torque had been implemented on the half of the steer by wire linked to the handlebar as well. This time the role is slightly different, since the handlebar is directly connected with the rider and all corrections are performed through the forces he applies while riding with his hands. What is important here is the consideration of not only the torque feedback coming from the motor but furthermore all the handlebar contribution. The initial configuration on SIMPACK have been modelled in a marginally different yet more complete way (*Figure 17 (a)*) to have a clear visual split between the top and the bottom part, even though a second version of it with rearranged position and exact distances have been already conceptualized *(Figure 17 (b))*.

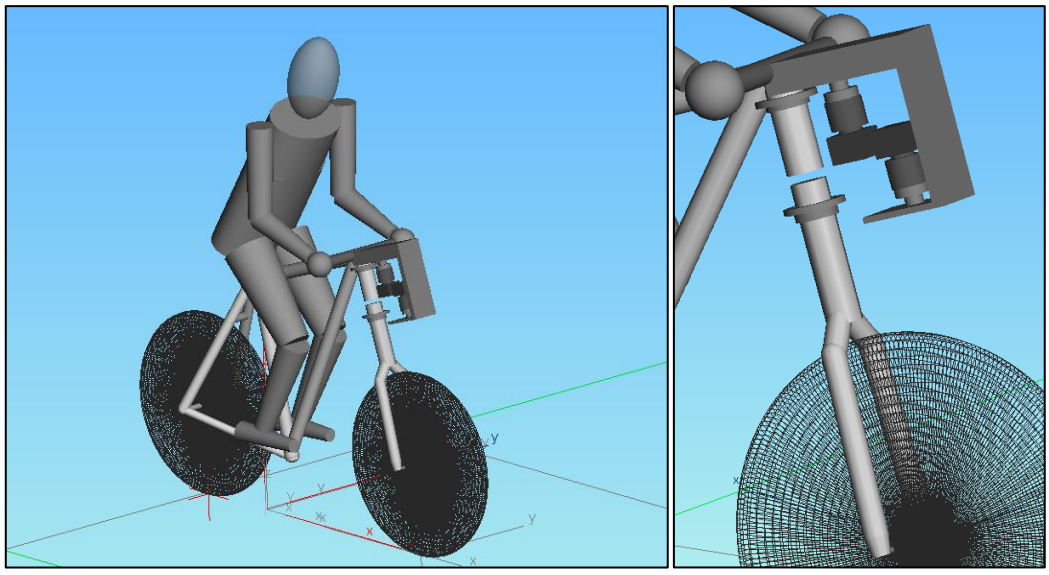

(a)

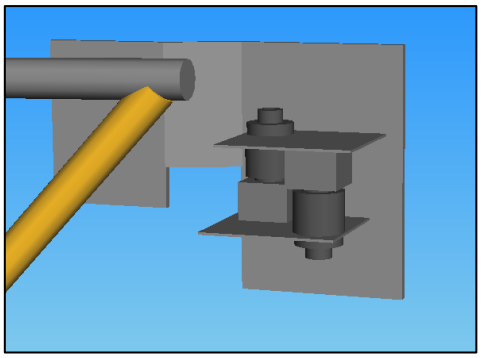

(b)

Figure 17: New installed Steer by Wire system on the model.

4. STABILISATION - CONTROL DESIGN

What is necessary now to make the steer by wire system start working is an adequate control strategy and control law to succeed in the goal of stabilisation. The subsequent steps refer to the understanding and utilization of MATLAB-Simulink as a tool to set to the side of SIMPACK to obtain the necessary torque produced by the motors. In this phase the rider will be supposed as a rigid body not acting on the dynamic of the bicycle with any force input since the only stabilisation effect on the lower part of the fork will be considered.

4.1 BASELINE OF THE CONTROL STRATEGY – Pole Placement

The focus is now shifted on a linear four degree of freedom model of the bicycle on MATLAB.

The strategy used here relies on the "Pole Placement method". The Full State Feedback or Pole Placement method is used in this case to place the poles of the closed loop system in a predetermined chosen location within the complex plane. Its main role is to stabilize a given system by ensuring that all closed-loop eigenvalues reside in the left half of the complex plane. Essentially, the location of the eigenvalues or poles affects the dynamic behaviour of the vehicle; this is characterized by the state matrix A, where the eigenvalues and eigenvectors affect its physical reaction to specific inputs. Because the state matrix depends on the bicycle's characteristics, changing its elements – especially the eigenvalues or poles – leads to different dynamics.

As a first step is necessary to take into consideration the linear Open Loop system in the state space form:

$$\dot{\boldsymbol{x}} = \boldsymbol{A} \cdot \boldsymbol{x}(\boldsymbol{t}) + \boldsymbol{B} \cdot \boldsymbol{u}(\boldsymbol{t})$$

$$\boldsymbol{y} = \boldsymbol{C} \cdot \boldsymbol{x} + \boldsymbol{D} \cdot \boldsymbol{u}(\boldsymbol{t})$$

Where $\boldsymbol{x} = [\boldsymbol{\varphi}, \boldsymbol{\delta}, \boldsymbol{v_y}, \boldsymbol{r}, \dot{\boldsymbol{\varphi}}, \dot{\boldsymbol{\delta}}]^{\boldsymbol{T}}$, **A** is the state matrix or system matrix, **B** is the input matrix, **C** is he output matrix and **D** the feed forward matrix or direct input-output gain matrix, with **u** as the input vector and **y** as the output vector.

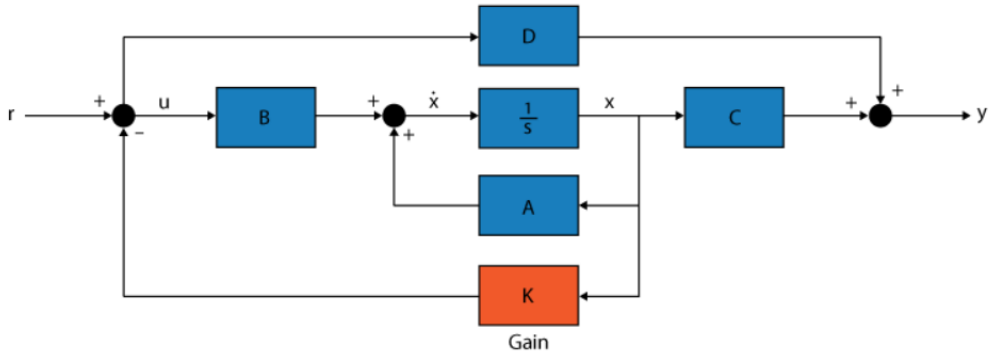

Figure 18: Pole placement block diagram.

Knowing that all the state variables are measurable and available for feedback and the system is completely state controllable, then the poles of the closed-loop system may be placed in any desired location, as said in (Levine, 2011). This condition translates in the rank of the controllability matrix **q** being equal to **n** (parameters):

$$\boldsymbol{rank}[\boldsymbol{B}|\boldsymbol{AB}|\ldots|\boldsymbol{A^{n-1}B}] = \boldsymbol{q} = \boldsymbol{n}$$

Which means that all the eigenvalues of the matrix **A - BK** can be controlled by state feedback, with **K** being the state feedback matrix. Since **A** and **B** depends on velocity, it is important to assess the controllability of the system as done in (Johannes Edelmann, Martin Haudum, Manfred Ploechl, 2015) not to incur in uncontrollable speeds. This is one first reason why the subsequent tests will start from taking into account speeds over 1.5 m/s.

Then after these considerations, the Matlab function "*place*" gives the six gain values to put in **K** after having chosen the desired pole position, to obtain a new Closed Loop system in the state space form:

$$\dot{\boldsymbol{x}}(\boldsymbol{t}) = \boldsymbol{A} \cdot \boldsymbol{x}(\boldsymbol{t}) + \boldsymbol{B} \cdot \mathbf{M}_{\boldsymbol{\delta}} = \boldsymbol{A_{CL}} \cdot \boldsymbol{x}(\boldsymbol{t})$$

$$\boldsymbol{y} = \boldsymbol{C} \cdot \boldsymbol{x} + \boldsymbol{D} \cdot \mathbf{M}_{\boldsymbol{\delta}} = \boldsymbol{C_{CL}} \cdot \boldsymbol{x}(\boldsymbol{t})$$

Having then finally **K** as a function of the speed:

$$\boldsymbol{K^T} = [\boldsymbol{K_{\varphi}}, \boldsymbol{K_{\delta}}, \boldsymbol{K_{v_y}}, \boldsymbol{K_r}, \boldsymbol{K_{\dot{\varphi}}}, \boldsymbol{K_{\dot{\delta}}}]^{\boldsymbol{T}}$$

Considering the equation of motion in state space representation, the torque $\mathbf{M_\delta}$ is:

$$\mathbf{M_\delta} = -\boldsymbol{K^T} \cdot \boldsymbol{x}$$

Where **K** is the gain vector obtained by the control law and **x** is the state vector defined before.

4.2 CONTROL STRATEGY - COSIMULATION

Having the **K** containing the gains to be multiplied by the correspondent six states in **x**, the control strategy holds the role to provide the feedback to the steer by wire system given the inputs contained in the state vector. This can be done thanks to a Co-Simulation environment (*Figure 19*), SIMAT, between SIMPACK and MATLAB-Simulink, where the first gives out the six states $[\boldsymbol{\varphi}, \boldsymbol{\delta}, \boldsymbol{v_y}, \boldsymbol{r}, \boldsymbol{\dot{\varphi}}, \boldsymbol{\dot{\delta}}]$ and the second receives these as an input and provides the output torque $\mathbf{M_\delta}$ (input in the Multibody System) after the computation. Briefly, SIMPACK solves the mechanical system and reacts to the control loop MATLAB solves.

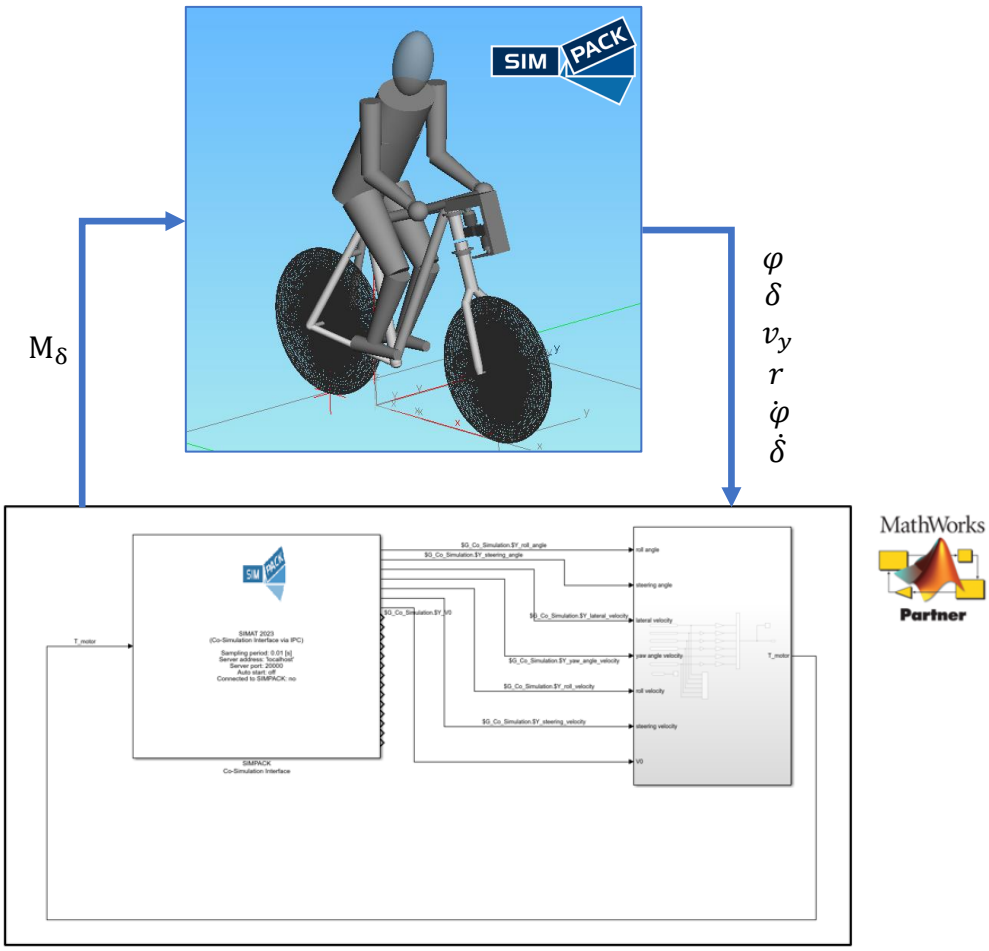

Figure 19: Co-Simulation environment.

It is fundamental to understand how the control design in Closed Loop will affect and correct the behaviour of the vehicle in case of some initial instabilities; hence, the Open Loop response will be analysed first to identify from which speed conditions the steer by wire system is needed the most.

4.2.1 OPEN LOOP RESPONSE TO INSTABILITIES

As said in *3.3* the bicycle has been tested for a set of different speed to be able to carry out the representation of the system through the eigenvalue plot. Now it is useful to look at the reaction of the system to an initial instability of 10° of roll angle (***φ***) at different decreasing speeds (*Figure 20*):

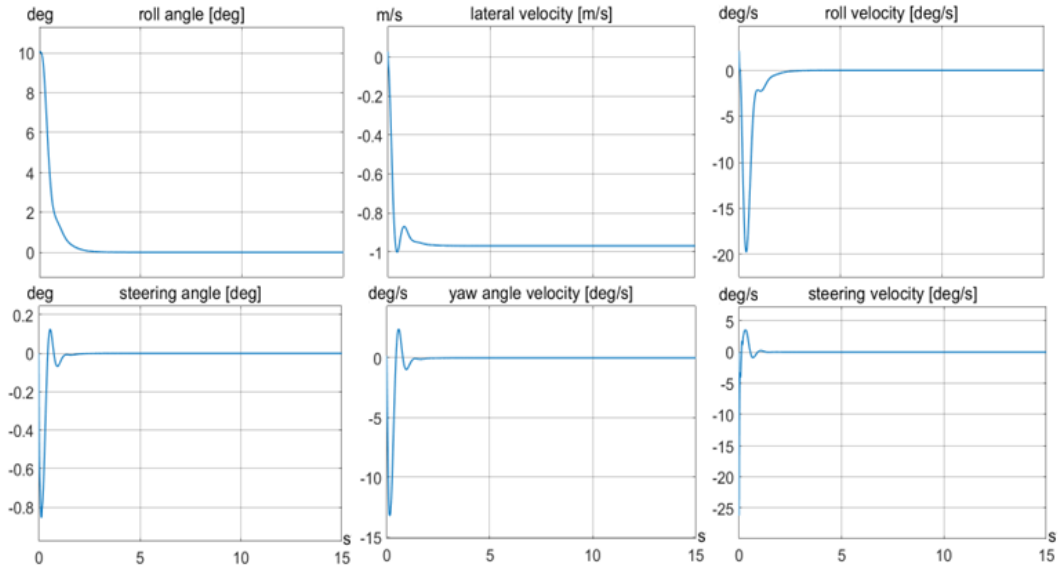

a)

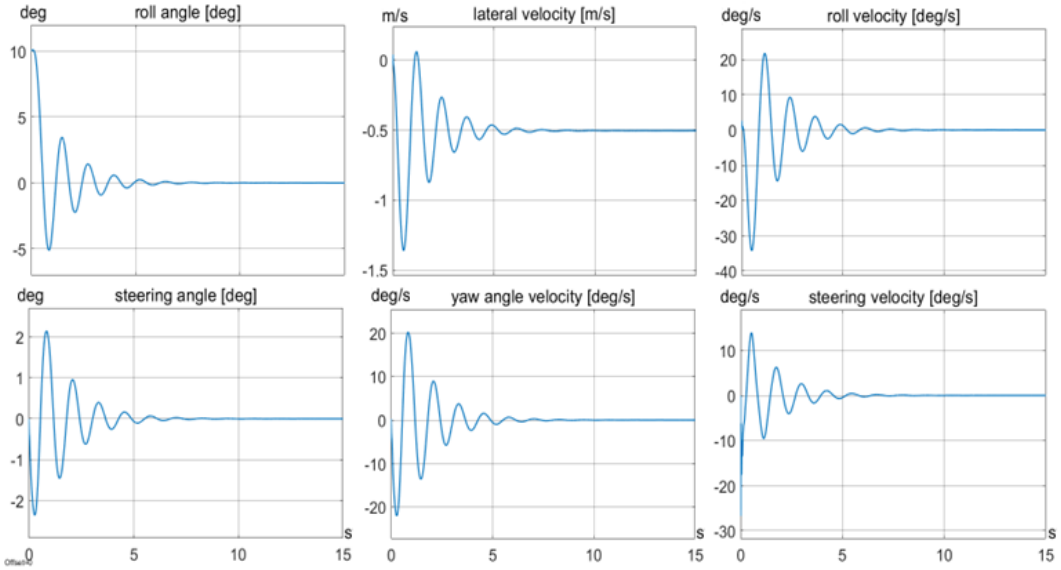

b)

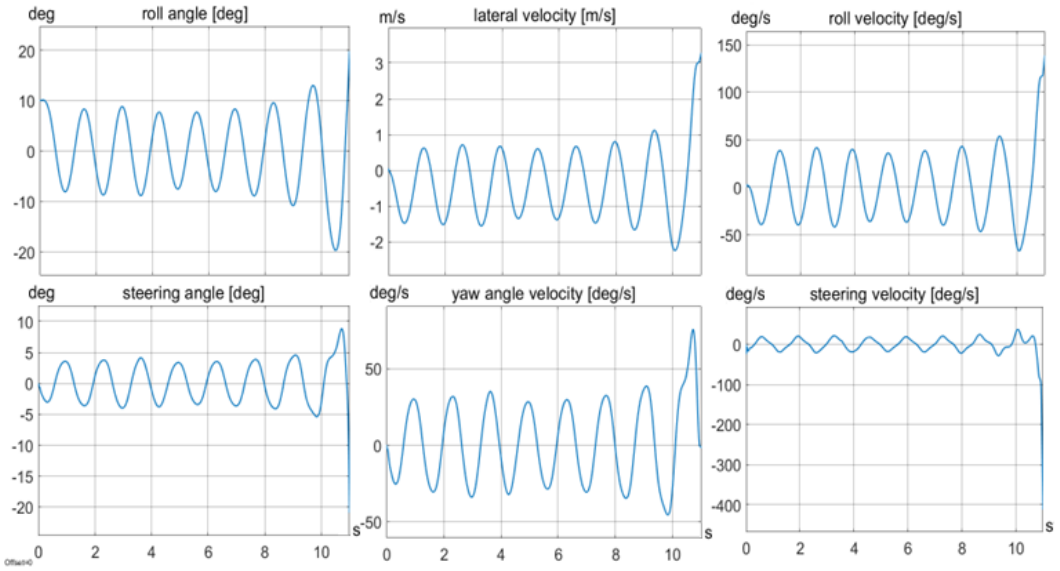

c)

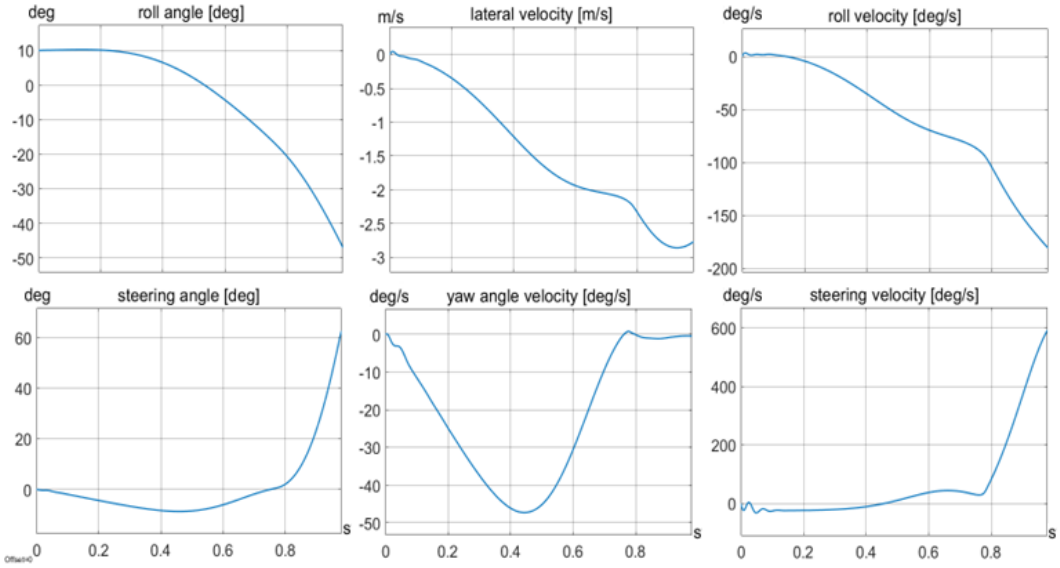

d)

*Figure 20: Bicycle behaviour with an initial instability of 10° **φ** at: a) 16 m/s, b) 10 m/s, c) 9 m/s and d) 6 m/s.*

The process of auto-stabilisation occurs smoothly at higher velocities leading the vehicle to set again in a stable and upright position in less than 3 seconds, free of any oscillation of the roll angle, for 16 m/s while a fast steer correction occurs in the beginning. For the case of 10 m/s the bicycle oscillates sideways and steers correspondently, reducing progressively the lean angle until regaining balance after almost 7-10 seconds. However, instability begins to escalate with exponential growth once speeds hits values below 10 m/s, eventually reaching critical levels and resulting in a toppling over after 11 seconds at 9 m/s, weaving constantly

around the upright position. This trend increases as velocity decreases, with oscillation disappearing below 6 m/s. The more the initial disturbances, the higher the speed necessary to keep the bicycle in the auto-stable speed range. So, at low speeds, the bicycle is more and more unstable and require frequent corrections from the cyclist to avoid an excessive side lean. However, at higher speeds, the inertia of the bicycle and its components (centrifugal force, vehicle dynamics, and the gyroscopic effect of the wheels) can contribute to greater stability.

4.2.2 CLOSED LOOP CONFIGURATION – TWO FEEDBACKS

The control architecture built in Simulink has the initial role of providing the feedback torque to the motor linked to the lower part of the fork. This is carried out inside the Matlab Function block of *Figure 22* where the pole placement method is applied, and depending on the speed the model is running at, a different set of gains **K** is provided. What can be observed in *Figure 21* is the SIMAT block providing the data from SIMPACK trough a Server-Client connection and the six signals of interest, the rotating motor velocity, **V0**, the forward velocity, useful to have a close look at it and how it changes during the trajectory corrections and two handlebar states which will be used further on in the analysis of the handlebar tracking control. Inside the control subsystem the control law explained in *4.1* is designed.

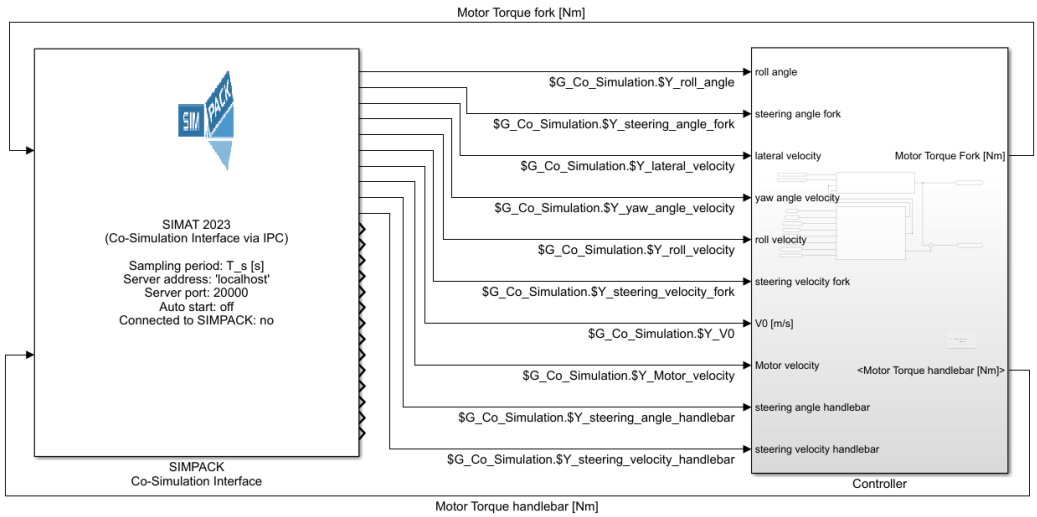

Figure 21: Simpack-Simulink communication interface on Simulink.

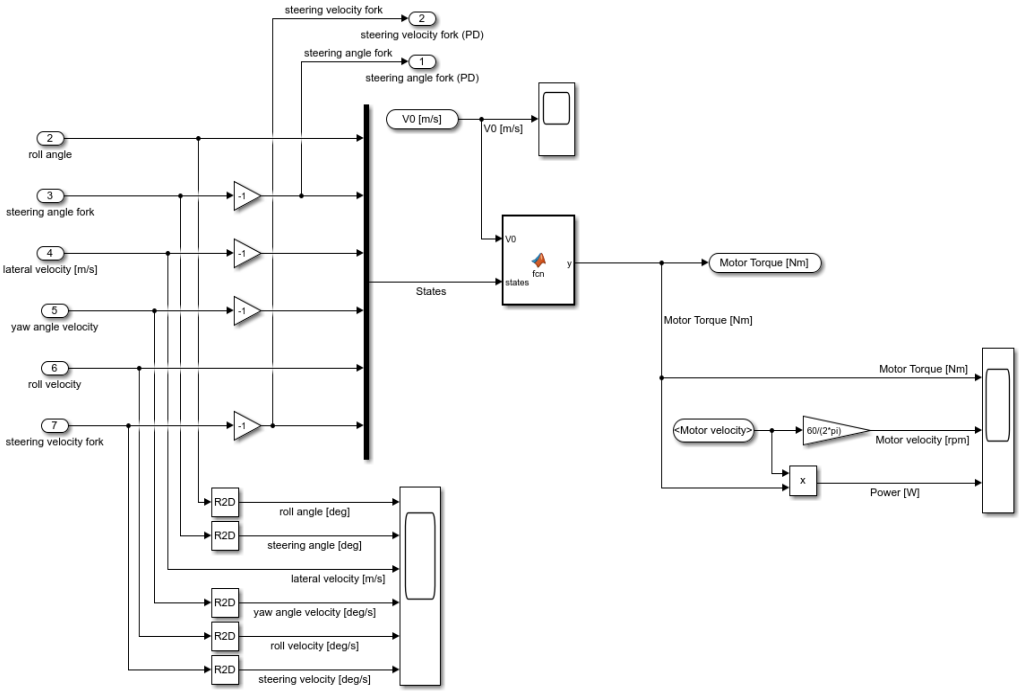

Figure 22: Simulink stabilization controller block diagram.

Following the work carried out by Limebeer and Sharp (Sharp D. J., October 2006) a first control strategy considered the only effect of feedbacking the roll angle ($\boldsymbol{\varphi}$) and the roll velocity ($\dot{\boldsymbol{\varphi}}$). To demonstrate the feasibility of the project and his consequences on the bike, this approach is applied to the same cases considered for the Open Loop system; the results can be observed in *Figure 23*.

Firstly, it is clear how the system managed to stabilise the vehicle at all the speed considered within a reasonably short frame-time and with a similar trend of response, even though a component of lateral velocity remains which causes a change of lane with respect to the straight line one of the start, highlighting the need of a more complex and complete form of controller to keep the bicycle in lane at the same time.

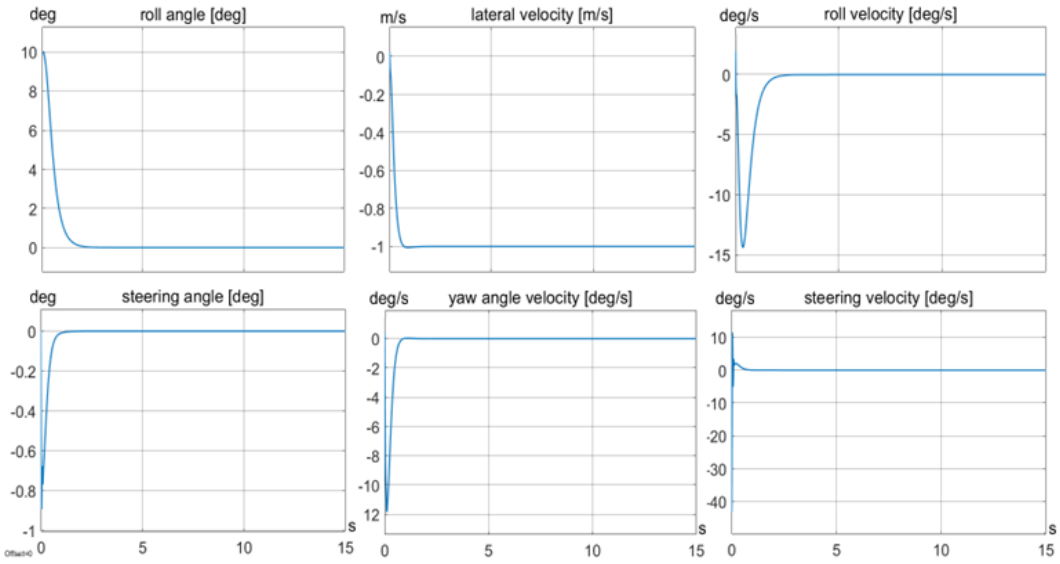
deg
roll angle [deg]
m/s
lateral velocity [m/s]
deg/s
roll velocity [deg/s]
deg
steering angle [deg]
deg/s
yaw angle velocity [deg/s]
deg/s
steering velocity [deg/s]
s

a)

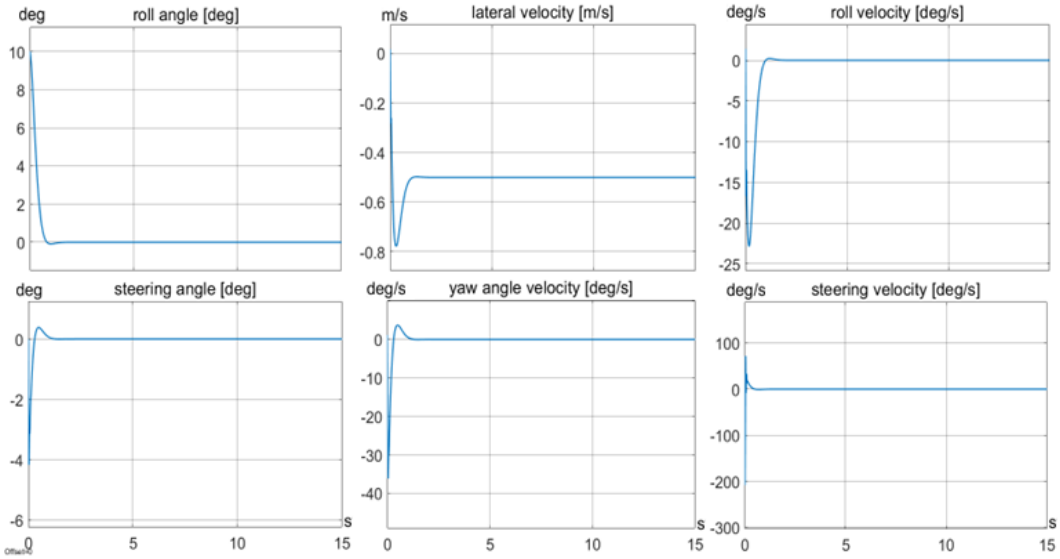
deg
roll angle [deg]
m/s
lateral velocity [m/s]
deg/s
roll velocity [deg/s]
deg
steering angle [deg]
deg/s
yaw angle velocity [deg/s]
deg/s
steering velocity [deg/s]
s

b)

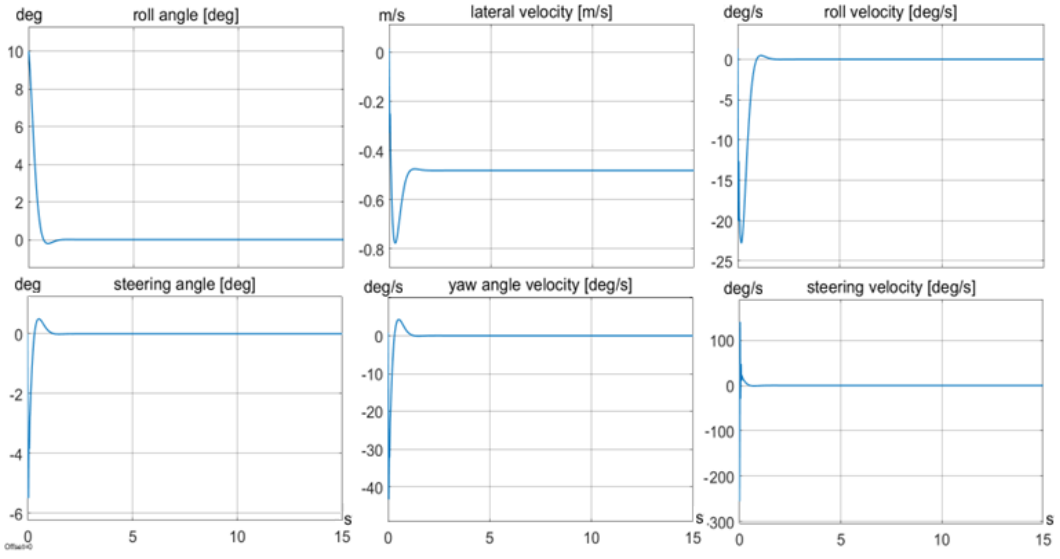
deg
roll angle [deg]
m/s
lateral velocity [m/s]
deg/s
roll velocity [deg/s]
deg
steering angle [deg]
deg/s
yaw angle velocity [deg/s]
deg/s
steering velocity [deg/s]
s

c)

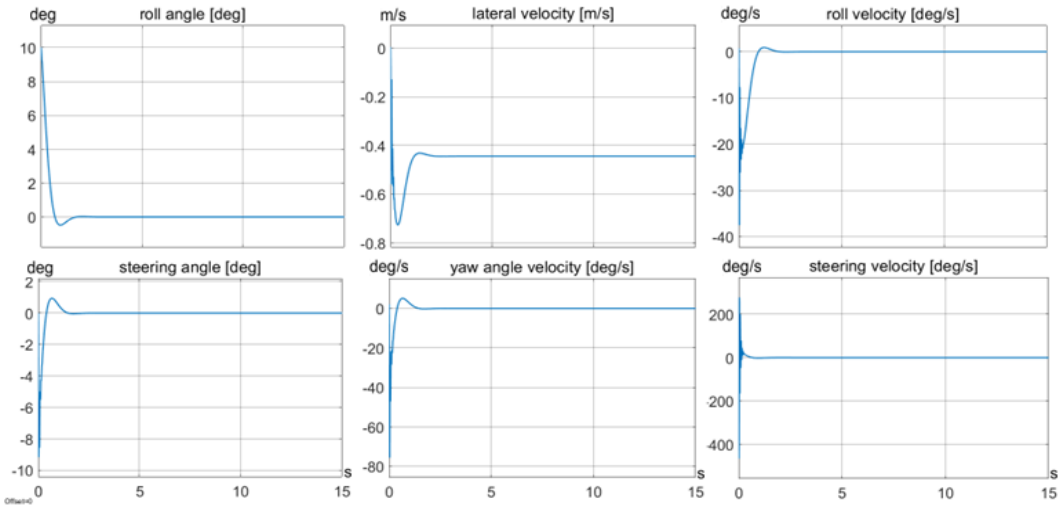

d)

Figure 23: Closed Loop system response to an initial instability of 10° $\boldsymbol{\varphi}$ with only $\boldsymbol{\varphi}$ and $\dot{\boldsymbol{\varphi}}$ in feedback for: a) 16 m/s, b) 10 m/s, c) 9 m/s, and d) 6 m/s.

However, it is noteworthy the existence of an inverse relationship between speed and the magnitude of torque required to correct instabilities. As speed decreases, the peaks in torque necessary for stabilization tend to rise. This phenomenon happens because of the direct transmission of torque $\mathbf{M_\delta}$, from the motor to the fork via the gearbox and pulleys. Consequently, this torque applies a proportional influence on steering velocity. At higher velocities, the bicycle benefits from auto-stabilization, necessitating less torque for stability maintenance, while at lower velocities the role of human corrective measures would increase, leading to a higher reliance on $\mathbf{M_\delta}$ to compensate for instabilities. It is also significant that at some higher speeds the influence of the steer by wire system interferes in a negative way with the self-auto-stabilisation, and this leads to longer responses in terms of time and the start of a slightly oscillatory behaviour.

This brings to the surface the matter of considering until which speed it makes sense to use the aid of the controller not to incur in loss of performance; this aspect will be subject to a more comprehensive analysis with the follow up of this case, considering the complete system with all six of the states in feedback. Basically, it is important to remind that the goal is to lower the effective range of stable velocity and enhance the stability in terms of a safe riding experience. It is for this reason and from (Johannes Edelmann, Martin Haudum, Manfred Ploechl, 2015), where it has been assessed 1.19 m/s as unstable velocity for a steering torque input, why from now on the focus will not consider under 1.5 m/s.

4.3 SIX STATES CLOSED LOOP - POLE PLACEMENT APPLICATION

After assessing the consistency of the controller even with a reduced quantity of feedbacks, the whole set of six states coming from the bicycle has been taken into account. From now on the discussion will proceed considering first the system in continuous time as it was first designed, analysing the response of the system at different velocities and disturbances, and evaluating how effectively the control strategy could help correcting instabilities from simple disturbances, then it will proceed discretizing it.

The objective of achieving stabilization has been pursued through the application, as said, of the Pole Placement method. However, clearing the practical implementation of this method and its consequential effects necessitates an explanation. As highlighted in *Section 3.3*, the positioning of eigenvalues in the complex plane bears significant influence on the dynamic behaviour of the bike system. Accordingly, their precise location has constituted the focal point of this analysis.

As stated in control methods literature, a first approach would be to "mirror" all the part of the poles holding a Real positive value, so that it can lay in the negative-stable side of the complex plane, without modifying the positive Imaginary part since it would be part of a complex conjugated pair and leaving the position of all the already negative part unfazed. Applying this method of proceeding brought the system closer to reach a stability, but it was not sufficient in a final analysis; hence, since it has been applied to multiple speeds and each one of them necessitated a different setting of parameters, further modifications have been applied. Initially, out of the six poles of the system (one for each state taken in consideration), only the two complex conjugated ones and the first only-real one have been modified, since they are the ones directly connected to the eigenvalue graph and the ones representing the trend of it (*Figure 24*), being the two non-real ones representative of the two overlaying weave modes and the first real one representative of the capsize.

4.3.1 SETUP OF TWO CONFIGURATIONS

This study chose to explore more combinations of parameters in view of having the possibility to utilize different settings for the same system. In fact, this is possible by choosing different pole locations, leading the system to behave differently in terms of response and intensity of the torque in output and in this case, two different solutions have been explored:

- For the first configuration, the emphasis is placed on achieving a faster system response to effectively counteract deviations from equilibrium, ensuring prompt correction of any disturbances. This leads the motor to exert higher torques since the gains coming from the pole placement method are higher in value, amplifying the feedback loop's influence. However, with the increased torque comes a higher energy requirement, necessitating considerations of power consumption and efficiency. This setup then prioritizes speed and agility, leading sometimes in high steering velocities which could result uncomfortable for the average driver.
- In contrast to the initial setup built towards a faster system response, the second configuration prioritizes stability and efficiency over speed. Here, the focus shifts towards creating a system with a slower reaction to instabilities, allowing for smoother and more controlled corrections. As a result, lower torque values are employed. This reduction in torque requirements contributes to energy-saving measures, increasing efficiency. It is worth of notice that achieving to have slower, yet less reactive system might imply the non-utility over certain speeds due to a faster response of the uncontrolled system due to the auto stabilization. This will be a matter of in-depth evaluation.

Seeing the representation (*Figure 24*) of what have been just said on the stability diagram with the eigenvalues could shed light the effects mentioned. It is clear how the first approach with the method effectively lowered all the eigenvalues on the complete interested speed range with respect to the uncontrolled model. It can also be considered consistent if compared with what have been obtained in (Pacejka, 2012) when performing a similar analysis on a motorcycle.

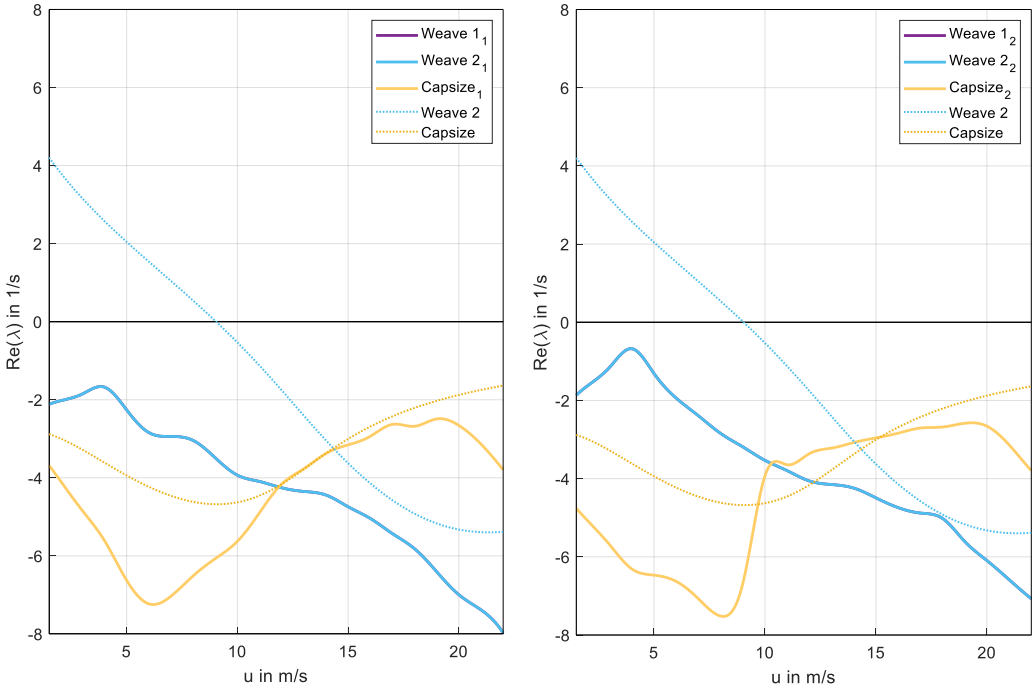

a)

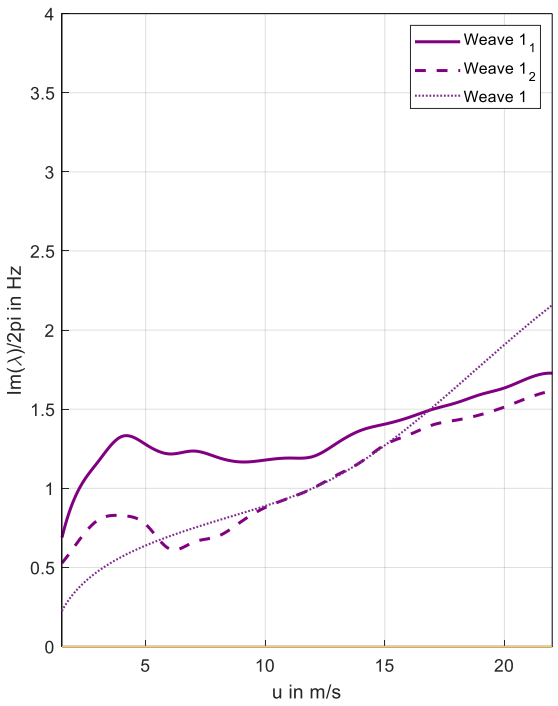

b)

Figure 24: Stability diagram showing the changes with respect to the (dotted) uncontrolled with first and then second setup of: a) Real part (first setup on the right and second setup on the left) and b) Imaginary part (first setup continuous line and second setup dashed line).

4.3.2 SIMPLE MANUEVERS AND DISTURBANCES RESPONSE

Investigating the practical implications of this strategy on the dynamic behaviour of a bicycle when correcting instabilities within a complex and varied environment is a hard task. Therefore, conducting initial trials with simple disturbances can show valuable insights.

The performance of the steer by wire bicycle underwent various testing across a broad spectrum of velocities, in a range from 1.5 m/s to over 20 m/s. However, the focus here lies in evaluating the system's capabilities under normal operating conditions. As such, attention will be directed towards analysing results obtained at velocities of 2 m/s (7.2 km/h), 6 m/s (21.6 km/h) and in some cases 10 m/s (36 km/h). The former represents a pertinent low-speed scenario characterized by severe instability, the second could represent a valuable similarity to the typical urban cycling speed, while the latter gives insights on a fast-cycling ride.

When selecting the type of disturbance, various inputs were examined to modify the system states in different manners, prompting diverse responses from the stabilization controller. Among the set of tests conducted, one particular observation merits initial consideration: the application of direct steering torque disturbance to the front wheel. Even though this was initially intended to assess the reaction to a sudden turn, this approach revealed a notable limitation. Upon closer examination, it became evident that the immediate effect of the motor receiving input torque signal to counteract instabilities resulted in torque being applied to the steering axis, consequently, any steering disturbance applied to this axis was quickly eliminated, rendering it unreliable for the analysis. As an example for this, it can be seen from *Figure 25* a disturbance 20 Nm Torque in input is precisely followed by both the setups without any noticeable difference while running at 6 m/s and subsequently to the end of it, the systems only takes few oscillations to nullify it.

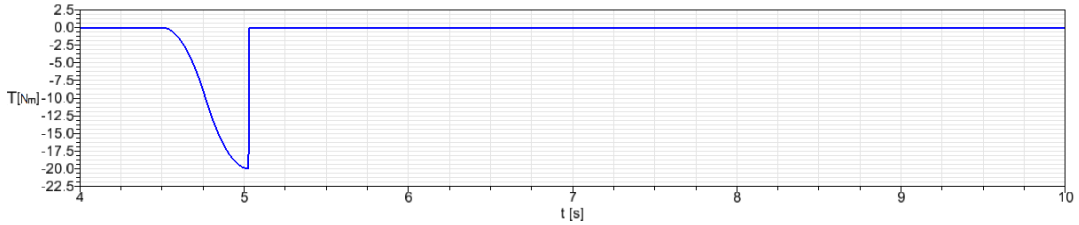

a)

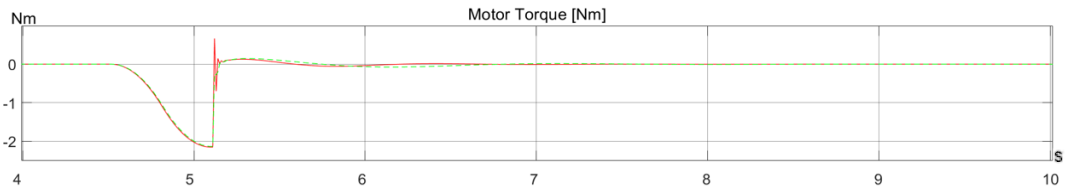

b)

Figure 25: 6 m/s run: a) 20 Nm steering torque disturbance input on the front wheel and b) torque response of the system for setup 1 (red line) and setup 2 (green dashed line).

Subsequently, a force of 200 N coming from a lateral direction and applied from 4.5 seconds to 5.1 seconds to the centre of gravity have been considered (see a graphical representation in *Figure 28*). This time the disturbance has been chosen for the impact it primarily has on the roll angle and on the roll velocity and its intensity able to cause the fall of the bike even if it was running at 10 m/s (autostability region). The system reacts promptly and manages to cope with the force in both cases and at all the speed considered; its lateral and steering performances can be seen in *Figure 26*. Here the black line represents the uncontrolled vehicle, the blue line the bicycle controlled through the first setup and the green dashed one through the second and slower setup.

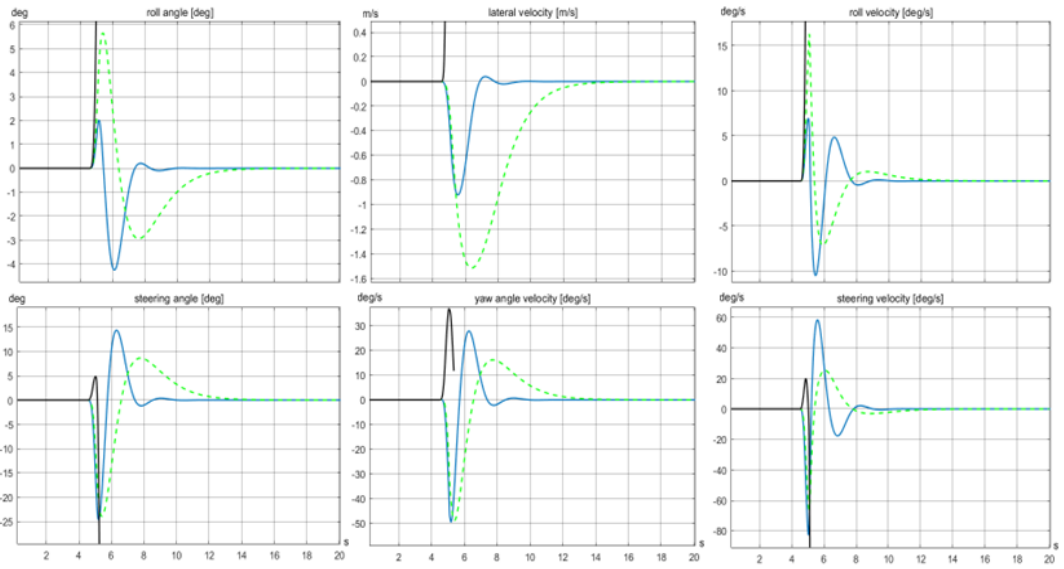

a)

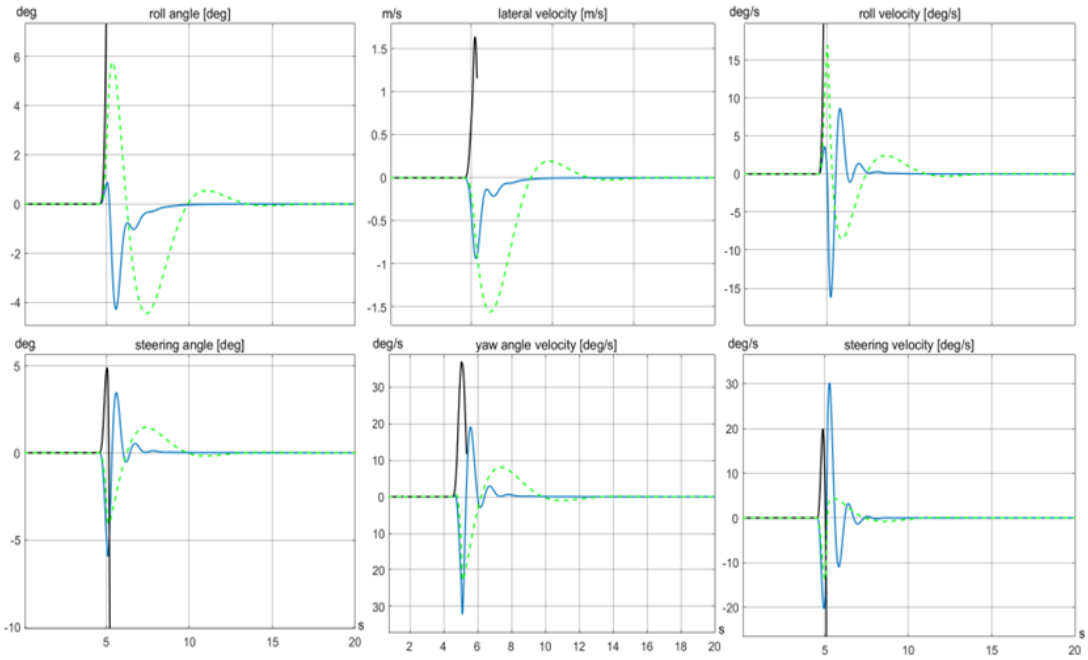

b)

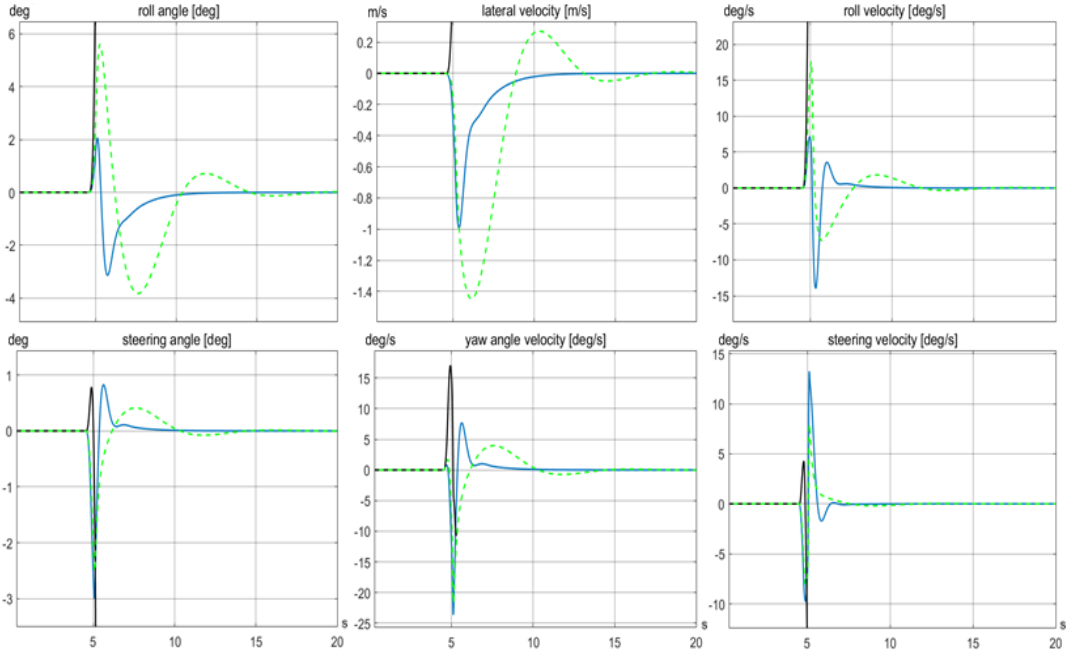

c)

Figure 26: States response graphs for the steer by wire bicycle a) 2 m/s b) 6 m/s and c) 10 m/s.

Initially, it becomes evident how the two setups operate differently and accordingly to the assumptions: the longer stabilization time arises by the smoother oscillations resulting in the system returning to balance and upright on average approximately 5 seconds later and with higher roll angle/velocity and lateral velocity peaks. Consequently, this leads the steering responses, both for the steering angle and steering velocity, to generally reach lower values, since a less intense effort from

the motor is required. In fact, this phenomenon is further reflected in the torque demand for each scenario and will be matter of considerations as well when the responses motor wise will be analysed. Turning the attention on the influence of the increasing speed, two aspects can be clearly observed: firstly, oscillations and the time required to restore equilibrium post-disturbance decrease in tandem with velocity increments; secondly, the steering effort decreases with the same trend. Both these outcomes are attributed to the auto-stabilization effect intensifying as speed increases, as previously outlined in *Section 4.2.1.*

Moreover, it is worth to focus also on the comfort aspect a rider will experience while riding a bicycle with an auto stabilizing system like this one. Clearly, while the first setup offers better lateral instability correction time response, a pertinent question arises regarding whether the system's responsiveness might be perceived as overly brisk or overly nervous by the rider. Here it comes the second setup, providing a smoother time response sacrificing some promptness. This distinction becomes clear when looking specifically at the steering feedbacks, at how the steering angle returns to the 0-degree position and with which velocity this happens; the sensation the driver feels could lean towards an uncomfortably rapid correction on one side or oscillating on the other side. The threshold between what is better between these two could both rely on the personal perceived comfort of the driver during the corrections or in the specific situation he will face, requiring greater or lesser quickness. This is surely an aspect the physical on-the-road tests will clarify.

As a general consideration for this first study, not only the disturbance here is minimized within a reasonably short timeframe, but also results in a marginal angular perturbation to the equilibrium state of the system at each velocity the test has been conducted. This serves as evidence of the efficacy of the control design and strategy employed.

Now, taking a look at the Torque in output from the controller (input for the motor) in *Figure 27* it is evident its decrement with the increment of the velocity. Not only the top values of the Torque diminish, but also the time the motor must impress it to stabilize is reduced, for both setups, having this an influence on the overshoots after the input disturbance.

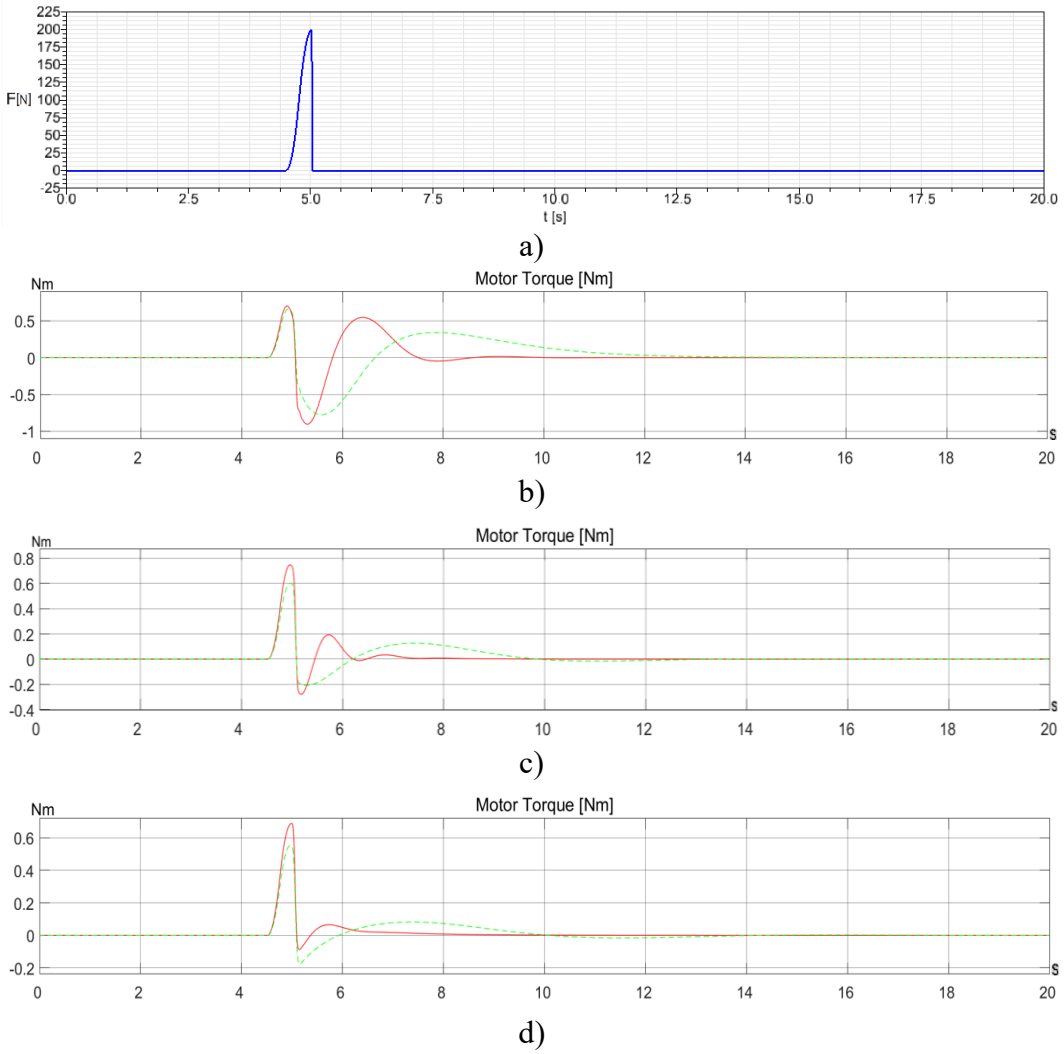

Figure 27: a) 200 N input disturbance Force and response Torque of the motor for: b) 2 m/s c) 6m/s and d) 10 m/s. The red line represents the first setup, the green dashed line represents the second, slower one.

A second disturbance applied for the same frame of time, from 4.5 to 5.1 seconds again to the centre of gravity, consists in a 50 Nm torque around the z axis made up to affect the yaw angle primarily and simulate one of the components that characterizes a slalom.

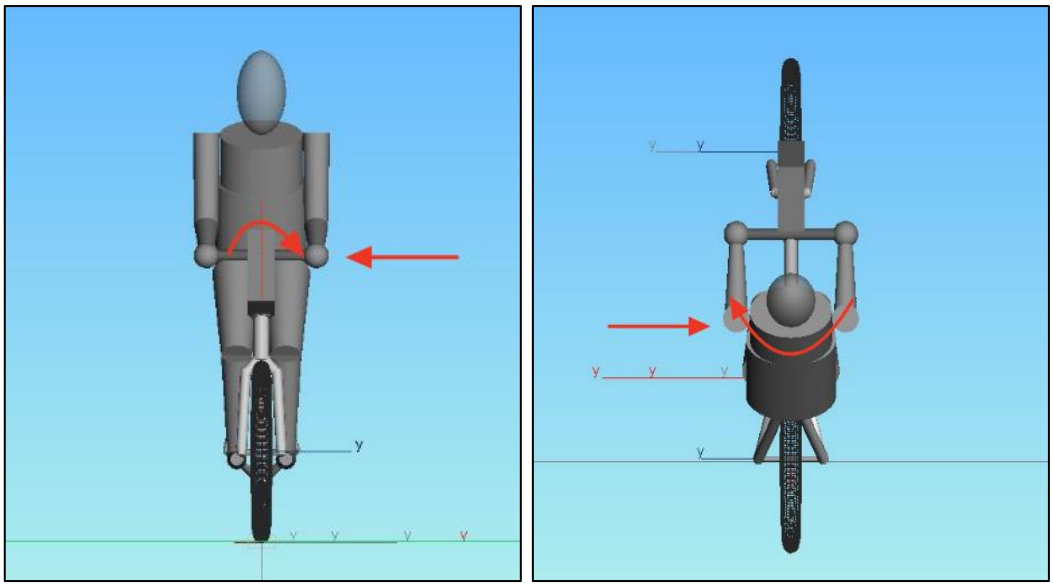

Figure 28: Representation of the simple Force-Torque disturbances applied on the bycicle.

Here the behaviour through the increment of speed is generally consistent with the previous case of the lateral push force, so it will be shown the effect of the steer by wire on the bicycle running at 2 m/s (*Figure 29*).

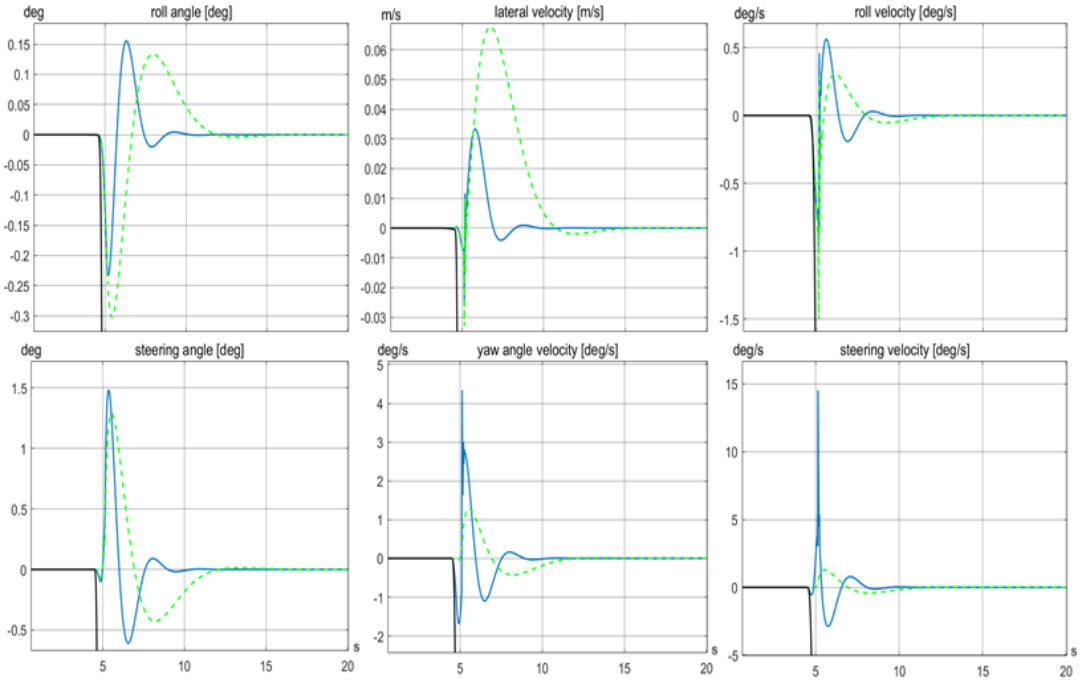

a)

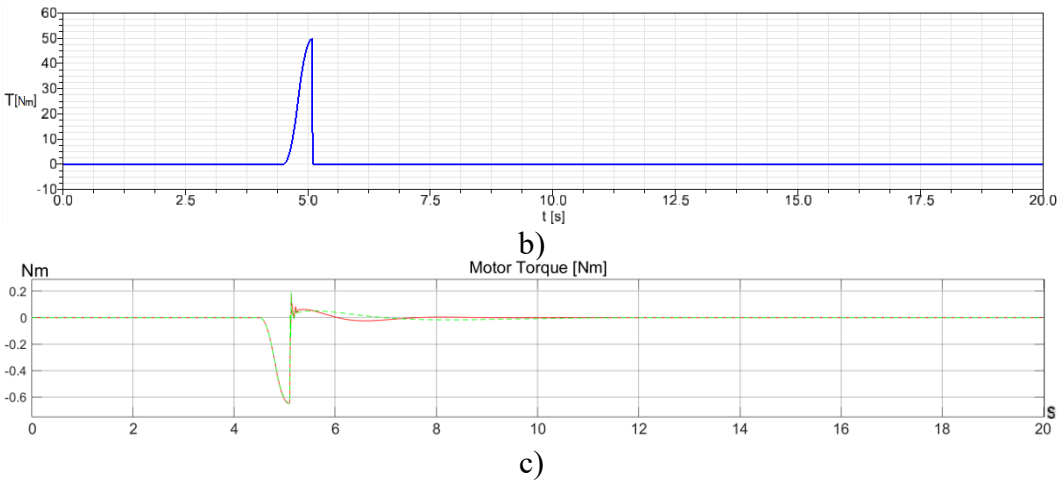

Figure 29: Yaw torque disturbance representation at 2 m/s through a) feedback states response, b) input disturbance torque and c) response torque of the motor.

Thus, it has been demonstrated that the application of an additional torque, derived from precise state information, can effectively expand the autostability domain. This guarantees that all eigenvalues have negative real parts over a wider spectrum of velocities. Consequently, the vehicle's controllability is significantly enhanced across various speed, with noteworthy improvements at lower velocities.

4.3.3 DISCRETIZATION

The process of converting continuous systems into discrete-time or discrete-space representations plays a fundamental role, facilitating numerical simulation, digital control algorithm development, and real-time processing on digital devices working at certain frequencies. Moreover, in applications where real-time processing is required, discretization serves to digital controllers and signal processing systems to operate on discrete-time signals allowing the use of filters that can be implemented in real-time hardware. Discretizing also opens for considerations on sensitivity analyses to be performed on the system: by discretizing it with different resolutions (sampling time), one can observe how this affects the behaviour of the response, which is crucial for understanding its robustness and sensitivity to parameter variations.

What it has been used in this Multiple Input case is the Zero Order Hold method (ZOH), which involves sampling the continuous-time signal at regular intervals and

holding each sample value constant until the next sample is taken, following the sampling time. This effectively converts the continuous-time signal into a piecewise constant approximation, where the value remains constant within each sampling interval. Let **u(t)** be the continuous-time signal and **u[k]** the "each sample value" entering the ZOH function, with **H(s)** the continuous system, the **y(s)** signal gives the discrete **y[k]** output when sampled every $\mathbf{T_s}$.

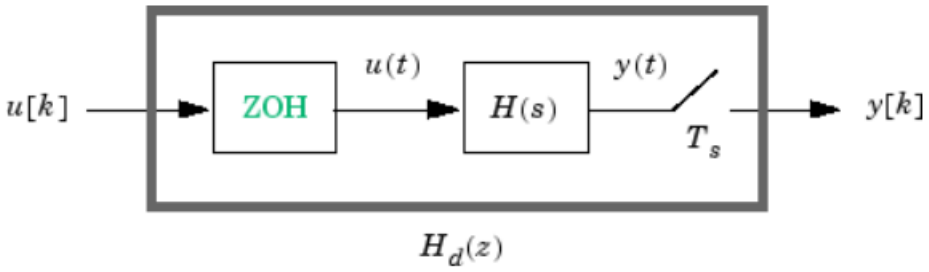

In this case a starting sampling frequency of 100 Hz is enough to make the discrete system follow the continuous performance without imprecision. The step-size is fixed and uniform.

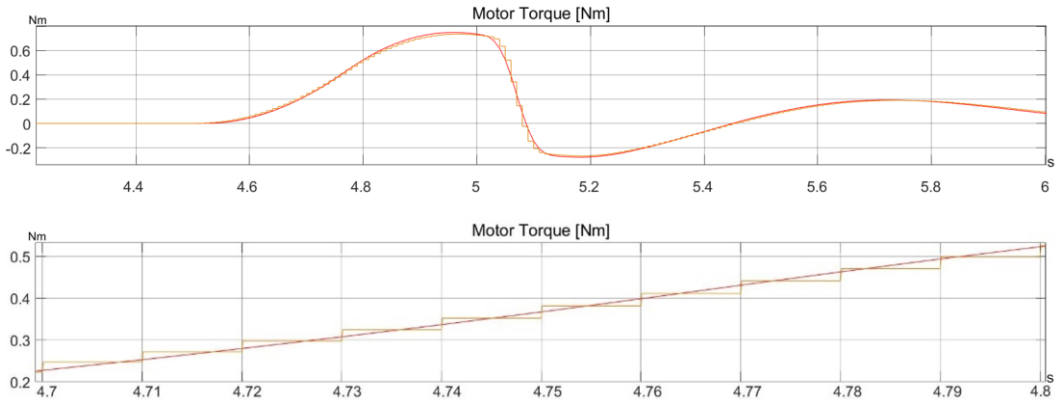

Figure 30: Discretized output torque at a sampling time of 0.01 seconds and a zoom for a frame of 0.1 seconds.

Here is shown how the Zero Order Hold method reduces the continuous signal to a stepped one at 100 Hz frequency. This one has been lowered until reaching a bad response and inconsistent stabilization at 70 Hz. Another impact the discrete Zero Order Hold method has on the system is related to the gains generated by the pole placement method. Since their value is affected by how precise the discretization method mirrors the continuous system, the more precise this process gets, the closer the gains will be to the continuous system one, hence without losing performances.

This is why, even after considering other approaches such as the First Order Holder (FOH) or the Tustin method (Franklin, 1997), the choice for the ZOH one has been privileged.

4.3.4 SYSTEM'S BEHAVIOUR OPTIMIZATION

At this point, having established the validity of the system in enhancing lateral stability, it becomes pertinent to explore ways for potential improvements of system performance. If looking at the eigenvalue plots of *Figure 24* the question about the region of validity and utilization arises. Observing the trends described by the two setups, the primary goal is to stabilize the trajectory of both in order to obtaining a homogeneous and steady one, preventing sudden shifts in behaviour from the vehicle during the transition from one velocity to another. Notably, within the velocity range of 1.5 m/s to 10 m/s, both setups demonstrate satisfactory operation; however, there is a potential risk of unpredictable speed fluctuations. The oscillatory behaviour observed in both modes during this range may contribute to such unpredictability.

Let's recognize as well that the two setups are designed to satisfy two different objectives: while the former aims to improve disturbances rejection and stability enhancement ensuring rapid responses in terms of time and a wider range of utilization in terms of speed, the latter is intended to help the rider to keep the bicycle upright during challenging and unpredictable manoeuvres especially at low speeds. Both should then converge towards the characteristics of the uncontrolled system at a certain velocity and become secondary (unutilized) to the auto-stabilization properties characteristics of higher speeds. It is for this reason that the imaginary part of the eigenvalue graph will be taken into account: the pole placement method will be used once again, now not to bring the system from an unstable to a stable situation, but to smoothen the trend of the control law in terms of eigenvalues. Here it follows how ideally this should happen (*Figure 31*).

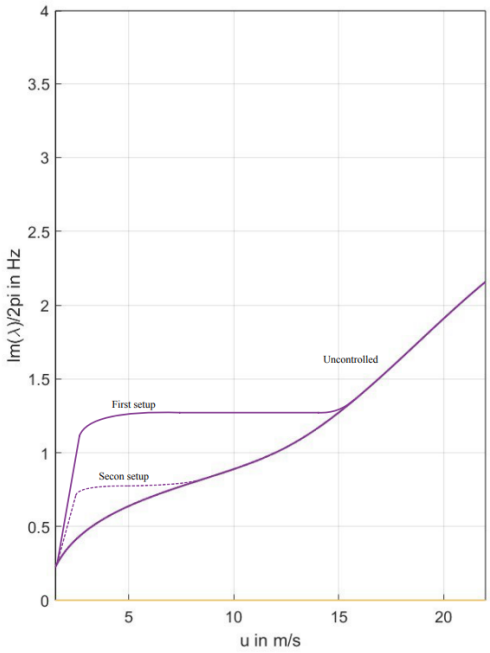

Figure 31: New ideal configurations, Imaginary part of the eigenvalue graph.

As previously said, a setup characterized by higher values (which will result in faster responses and bigger gains) with a wider speed range of utilization and a second less severe one have will be implemented.

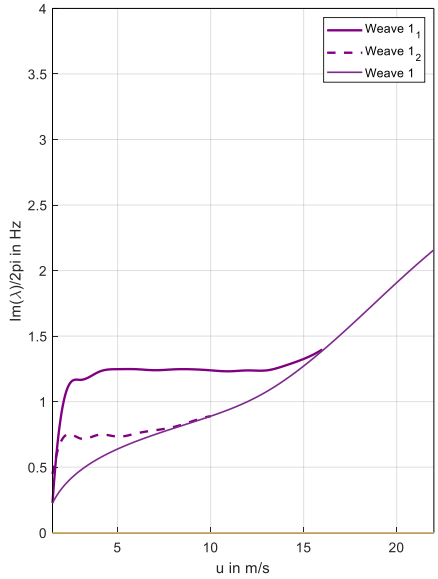

Figure 32: Imaginary part of the final two setups in a flatter and smoother fashion.

What comes out from re-placing the poles is a first configuration which works until 16 m/s and a second one that can successfully help in stabilizing until 10 m/s when it turns not to be useful anymore. In *Figure 33* also the real part has been displayed.

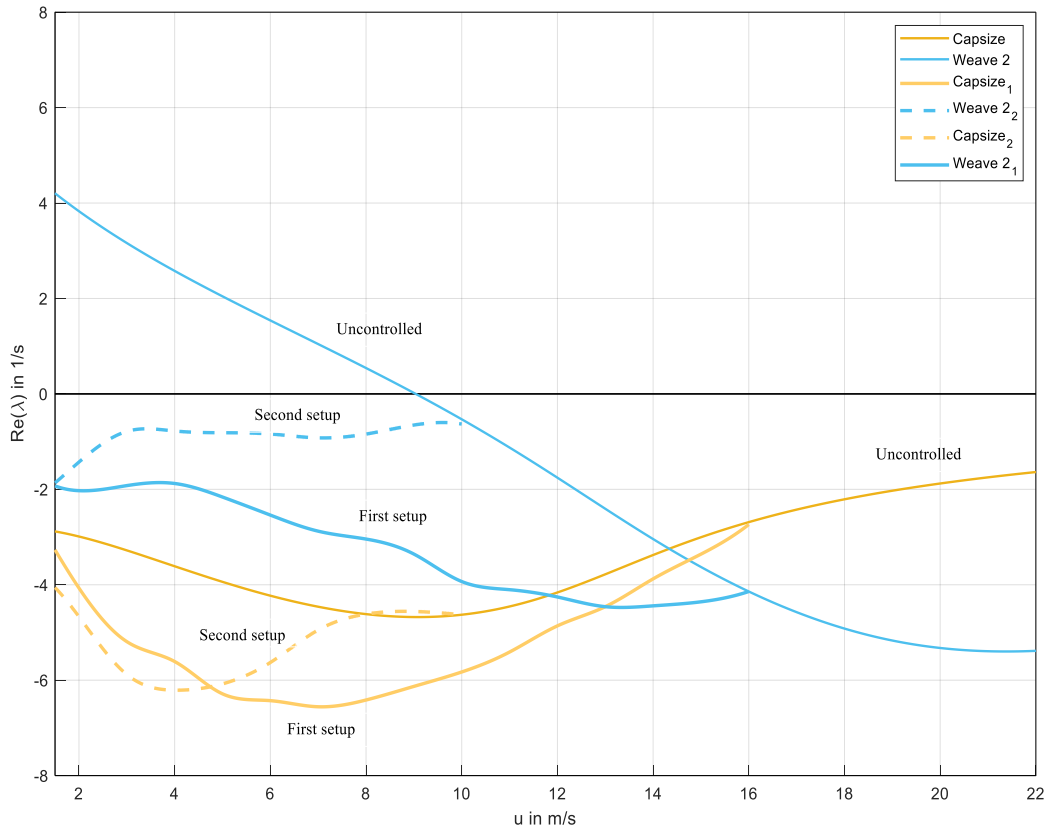

Figure 33: Real part of the final two setups in a flatter and smoother fashion.

Performances wise there has been low to no loss or decrease in terms of how fast the system was reacting at low velocities, here in fact the transition from one speed to the other didn't make any difference in those terms, it was in fact difficult to notice any substantial change in the trends when running the Co-Simulation.

The 6 gains which describe what is the influence of the pole placement controller on the steer by wire system for each velocity have been plotted in *Figure 34* over the range of speed considered. What can be clearly witnessed is, as expected, the strong influence at low speeds, especially from the roll angle and steering angle input, and the sensible decrease of the magnitude of the values between first and second setup, highlighting the difference in how effective the intervention between is the two.

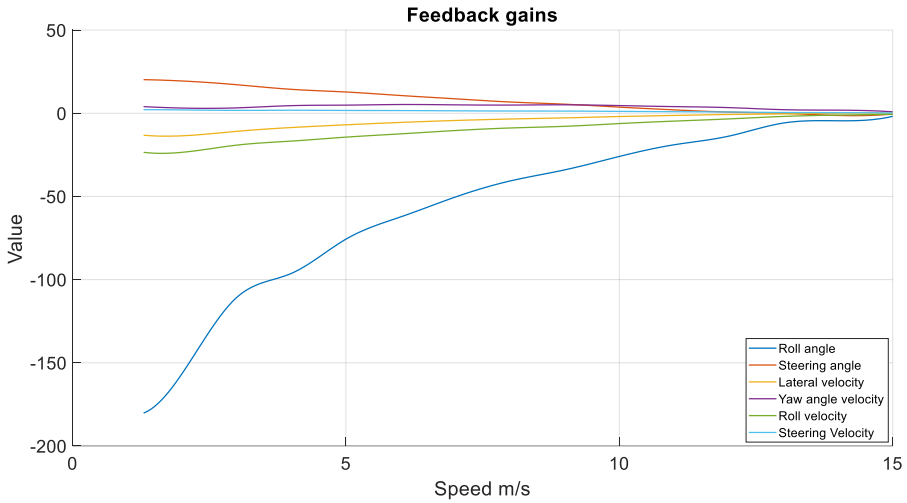

a)

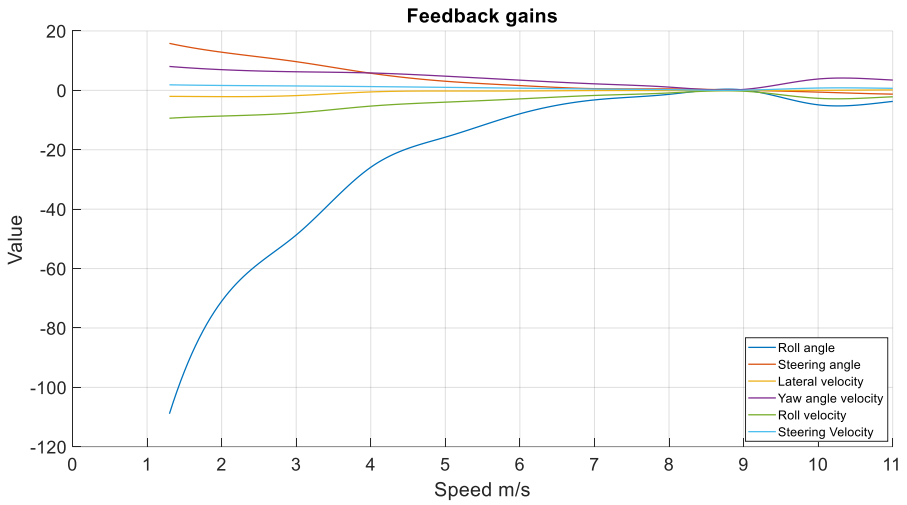

b)

Figure 34: Pole placement feedback gains for: a) First setup and b) Second setup.

Then, a more complete run able to detect the behaviour of the system now that it has been not only assessed as valid but optimized as well have been performed. Firstly, the controller has been modified to detect the actual, current velocity the bicycle is running at a certain moment and choose the set of gains calculated from the nearest integer speed to the one detected. This way the system could adapt during braking, accelerations, and speed change of every type.

4.3.5 COMPLEX MANUEVERS AND DISTURBANCES REJECTION

In order to completely test how the steer by wire system is stabilizing in a more critical situation, a dynamic speed transition run of 120 seconds have been carried on while persistent perturbations affect the lateral stability.

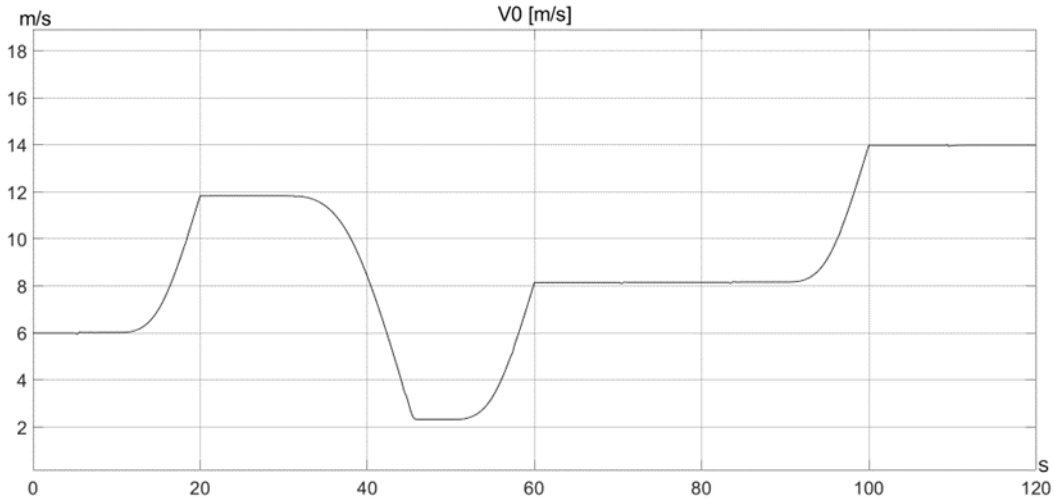

Figure 35: Forward velocity profile of the complete run for the first setup.

Starting from a baseline of 6 m/s with a first 10 seconds acceleration to bring the system to 11.8 m/s, to continue with a long, hard braking enduring for 15 seconds until reaching the low velocity of 2.3 m/s, accelerating for 10 seconds two times up to 14 m/s and completing the run after 2 minutes (*Figure 35*). During all this frame of time lateral forces (the same one analysed in *4.3.2*) from 180 N to 200 N disturbed the equilibrium of the vehicle by pushing it every 13 seconds, so actually perturbating it both during constant velocity cycling and speed transitions. It is worth to mention that lateral disturbances do affect the forward velocity **V0** because of a momentaneous modifications of the straight path, yet not necessarily enough to cause important changes in its trend (*Figure 36*).

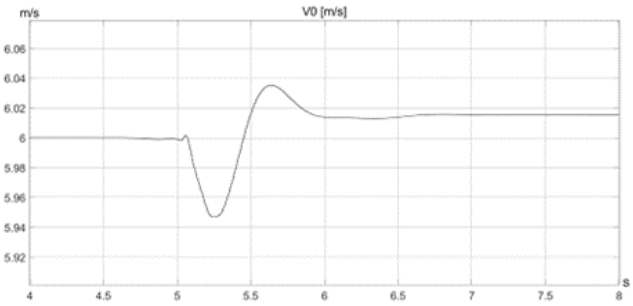

*Figure 36: Lateral disturbance influence on forward speed **V0** at 6 m/s.*

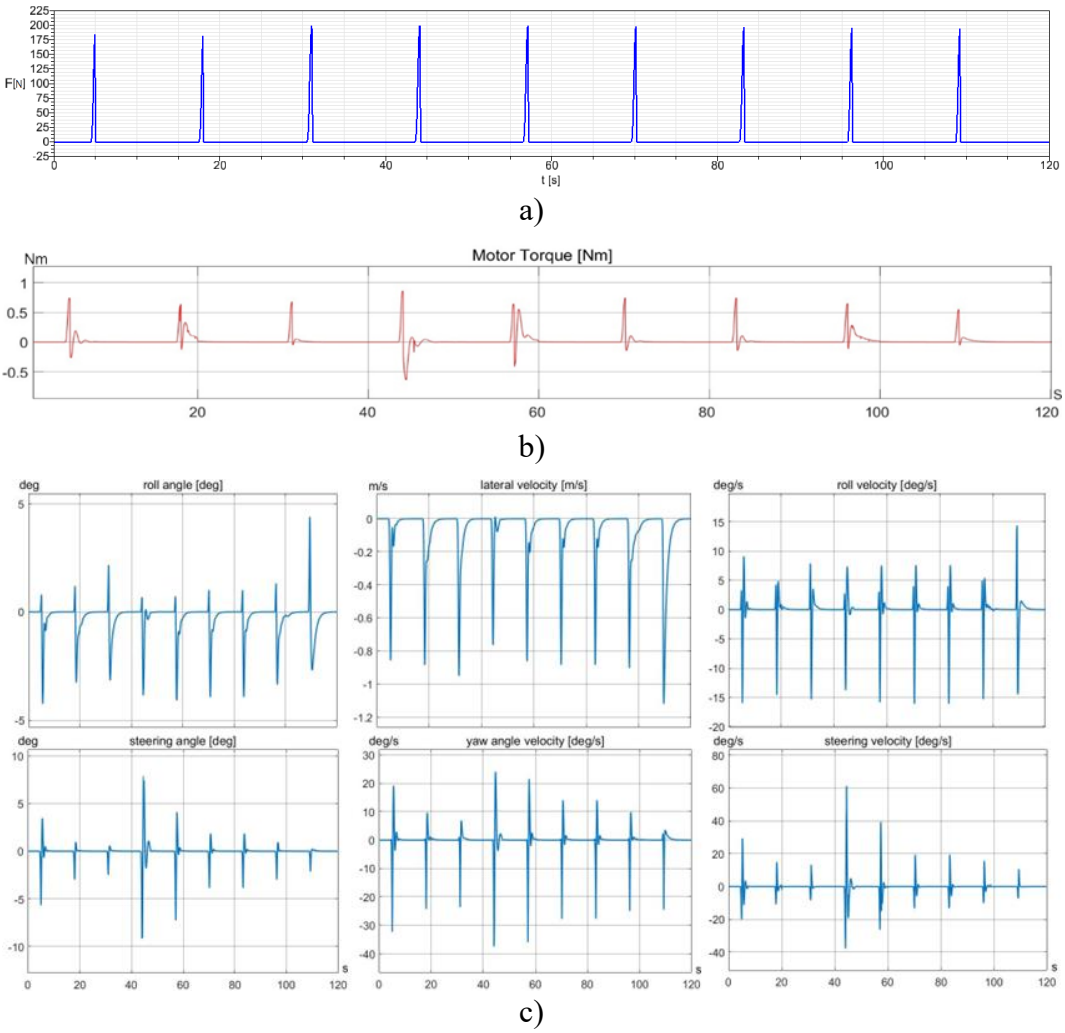

Figure 37: Bicycle response to manoeuvres from the a) disturbances: b) Motor response torque and c) six states in feedback during the corrections.

The obtained result is successfully aligned with the premises done in *4.3.4.* In fact, despite variations in speed across different phases, the lateral stability recovery in terms of roll angle and its velocity (*Figure 37*) along with the duration of the manoeuvre, remain consistent. This uniformity ensures that riders experience no abrupt changes in the behaviour of the steer by Wire system. This affirmation is

further supported looking at the response the motor exerts during each correction, since the Torque applied to the fork does not differ much during the run (*Figure 37*). Similarly, minimal deviation is observed in lateral velocity, indicating negligible influence on the vehicle's trajectory.

In contrast, the steering states and yaw angle velocity exhibit different responses depending on the speed: this is attributed to the auto-stabilization effect observer at higher velocities. Indeed, it is evident how when cycling at lower velocities (e.g., during the first, fourth and fifth disturbances) the steering effort and impact is greater than the ones occurring at higher speeds (e.g., from the sixth lateral push onwards). Furthermore, as speed approaches 16 m/s, the motor's involvement in the correction process diminishes. This becomes evident by looking again at the Torque at 14 m/s, being it lower and imprinting a minor correction input. Such behaviour aligns with the controller's design, which deactivates at higher, auto-stable speeds.

Let's a look at the run made up for assessing the proper functioning of the second setup (*Figure 38*). The configuration of the breaking and accelerations and their duration is the same as before during the whole 120 seconds duration, as well as the initial speed of the test, what changes is their intensity so that the speeds involved are the ones of the second setup.

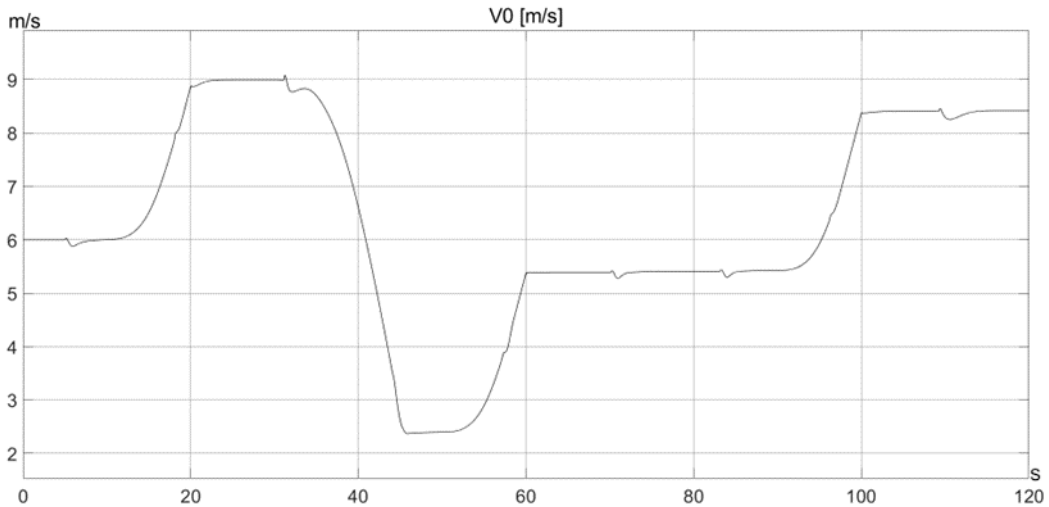

Figure 38: Forward velocity profile of the complete run for the second setup.

Another major change is the impact the disturbances have on **V0** this time, as it is visually clear how these will affect the forward velocity which will oscillate during the whole duration of the correction way more than it was happening before. This is caused by the highest impact on lateral stability the slowest setup has, influencing on the forward velocity as well.

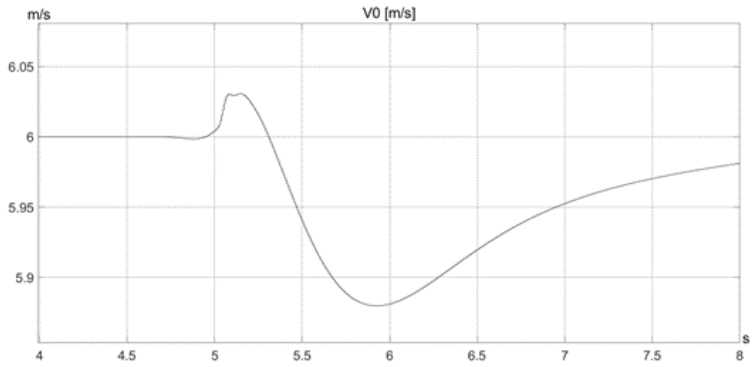

*Figure 39: Lateral disturbance influence on forward speed **V0** at 6 m/s.*

Again, in this case, the set of lateral disturbances is the same as the previous trial. However, their effects show notable distinctions from the first setup run, despite achieving complete correction across the entire speed spectrum under consideration. Notably, the response time for restoring the system's stability and the magnitude of lateral stability states involved in the manoeuvre (such as roll angle/velocity and lateral velocity) are heightened, especially when the configuration approaches its the upper limit of 10 m/s; it is at this threshold that the bicycle's behaviour aligns more closely with the uncontrolled scenario. This is particularly evident looking at the reaction at the third push to the system, where the three parameters mentioned above reach higher peaks with a subsequent lower torque from the motor.

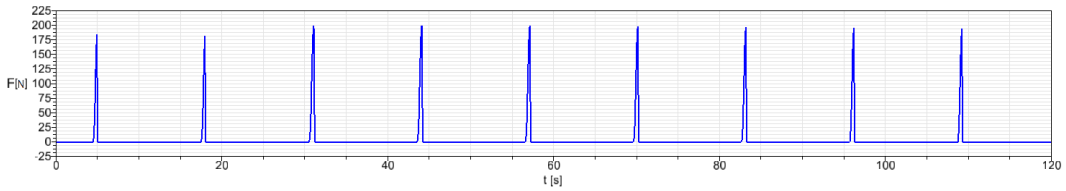

a)

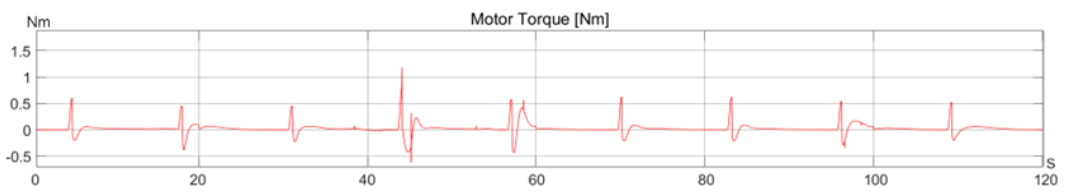

b)

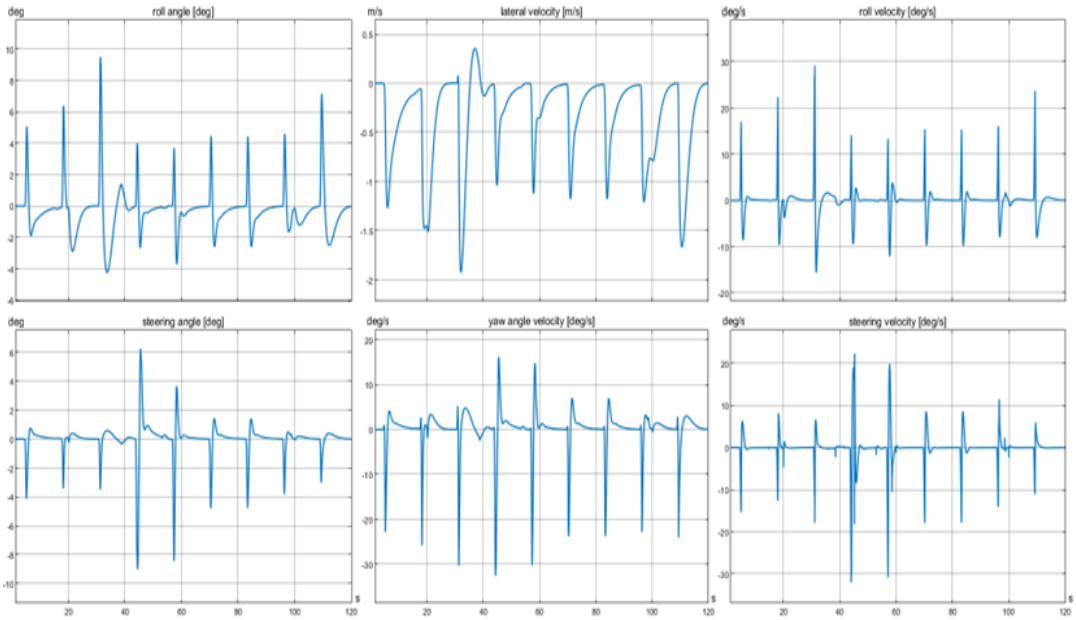

c)

Figure 40: Bicycle response to manoeuvres from the a) disturbances: b) Motor response torque and c) six states in feedback during the corrections.

Similarly to the preceding test, the higher the speed, the lower the torque required thanks to the auto stability of the vehicle; however, in this case, its requirements are generally diminished due to the setup's less intrusive and torque-efficient nature. One apparent anomaly could be attributed to the particularly high motor torque and subsequently steering states reaction when it comes to reject the fourth disturbance after 42 seconds: here the two effects of the lateral push and the ending of the breaking leads the instabilities to sum up and require a bigger effort to stabilize.

5. HUMAN-HANDLEBAR INTERACTION

In any biking situation, the rider utilizes the handlebar, applying forces traduced in torques on the steering axis, to command directional operations; therefore, the handlebar serves as the primary means to steer the bicycle in the intended direction. When facing any correction manoeuvre, the front wheel with all the steering elements will change their state in order to maintain the equilibrium; it is in this phase that the handlebar must cope with it and reproduce the exact movements to give the rider the sensation of a traditional mechanical connection as precise as possible. Simultaneously, it is of a main interest that the steering mechanism accurately follows the position of the handlebar, ensuring minimal deviation and delays in response.

It is in this chapter that the connection between handlebar and fork will be interrupted and the behaviour of the two will be as close as possible to the one of a mechanically linked bicycle thanks to a handlebar tracking control strategy.

5.1 HANDLEBAR TRACKING CONTROL

The handlebar tracking control strategy is set to minimize the error between the handlebar angle $\boldsymbol{\alpha}$ and the steering angle $\boldsymbol{\delta}$ with the minimal possible delay. This will be done by a PD controller designed to provide the torque $\mathbf{T_h}$ to the upper motor.

$$\boldsymbol{T_h = k_p(\alpha - \delta) + k_d(\dot{\alpha} - \dot{\delta})}$$

Where $\mathbf{k_p}$ is the proportional and $\mathbf{k_d}$ is the derivative gain. In this case they are chosen to be $\mathbf{k_p = 70\ Nm/rad}$ and $\mathbf{k_d = 0.3\ Nm.s/rad}$ to reduce the overshoot in the response and minimize the steady state error. This is possible because they are chosen such as a critically damped system response with equation of motion:

$$\boldsymbol{I\ddot{\alpha} + k_d\alpha + k_p w_o = 0}$$

With **I** inertia of the handlebar and $\mathbf{w_0}$ is the undamped natural frequency.

It is also a main interest not to rise the gains over a certain limit so that the oscillations which will occur in real life won't be amplified too much making the system unstable. Limiting the value of the gains means also keeping the value of the torque the motor exerts inside a certain bound.

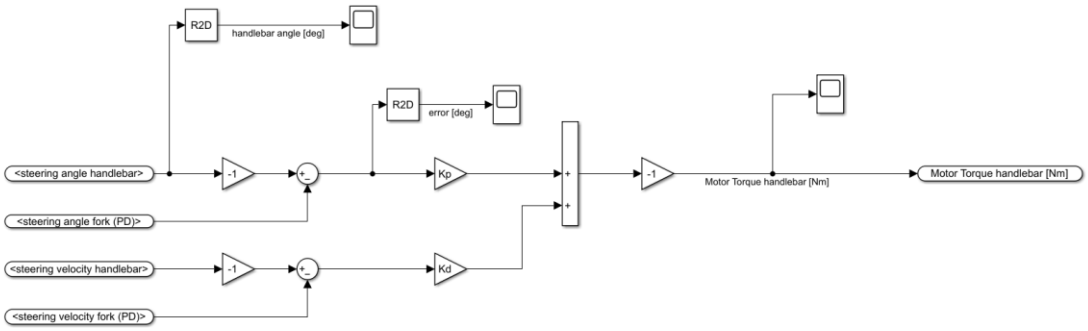

Figure 41: Handlebar PD tracking control block diagram on Simulink.

The error between the handlebar angle and steering angle is multiplied by the proportional gain and the same process for the handlebar angular velocity and steering velocity which are multiplied by the derivative gain. All these values are directly measured from the multibody system on Simpack, so it was not necessary to use any derivative block to apply on the angles to obtain the velocities. After summing the two contributes, the Torque $\mathbf{T_h}$ is obtained (*Figure 41*). When this tracking controller is active, it is necessary to raise the sampling frequency of the discretization to 150 Hz to ensure the system to work properly with the chosen gains.

Following in *Figure 42 a)* it can be noticed how the system works following the fork while the stabilisation control corrects the lateral instabilities of the first run shown in *4.3.5*. Here the focus is on how the handlebar can track the steering angle with the least possible error, without any force/torque applied on it. It can be seen in *Figure 42 b)* how the force is different and generally lower from the one in *Figure 37 b),* highlighting how the two motors work independently.

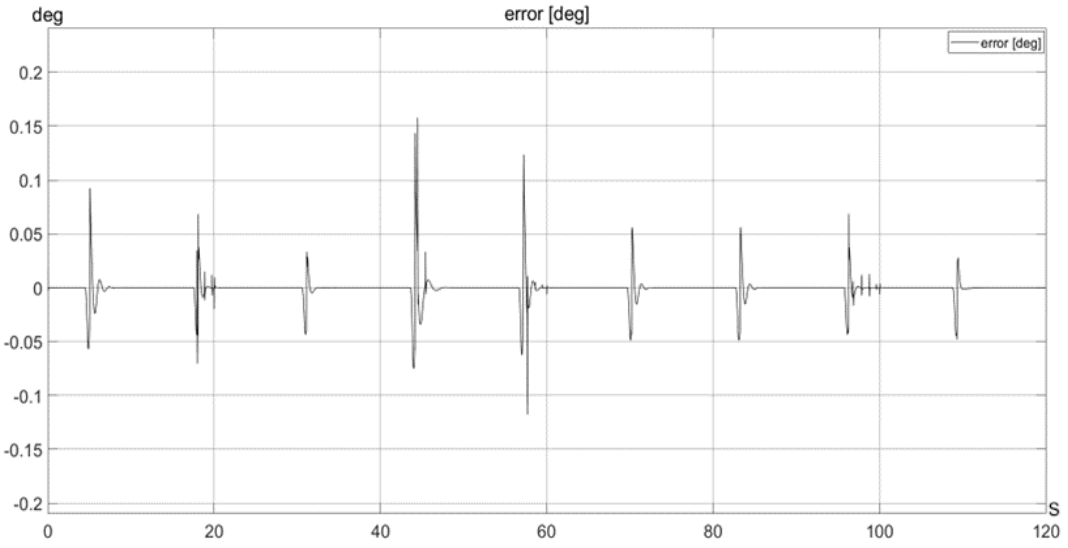

a)

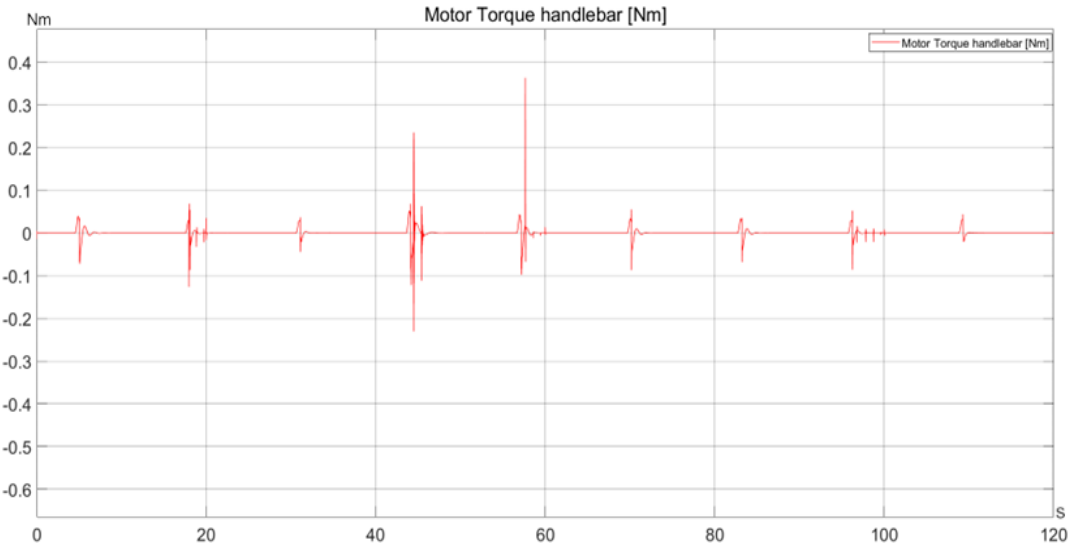

b)

Figure 42: a) error between handlebar angle and steering angle and b) torque applied by the upper motor as result of the PD controller.

5.1.1 EXTERNAL FORCE ON THE HANDLEBAR

It is from applying a force on the handlebar coming from the driver that is possible to witness if the system works both ways, so not only with the upper part following the stabilisation, but also allowing the fork to follow handlebar inputs while cornering or executing controlled manoeuvres.

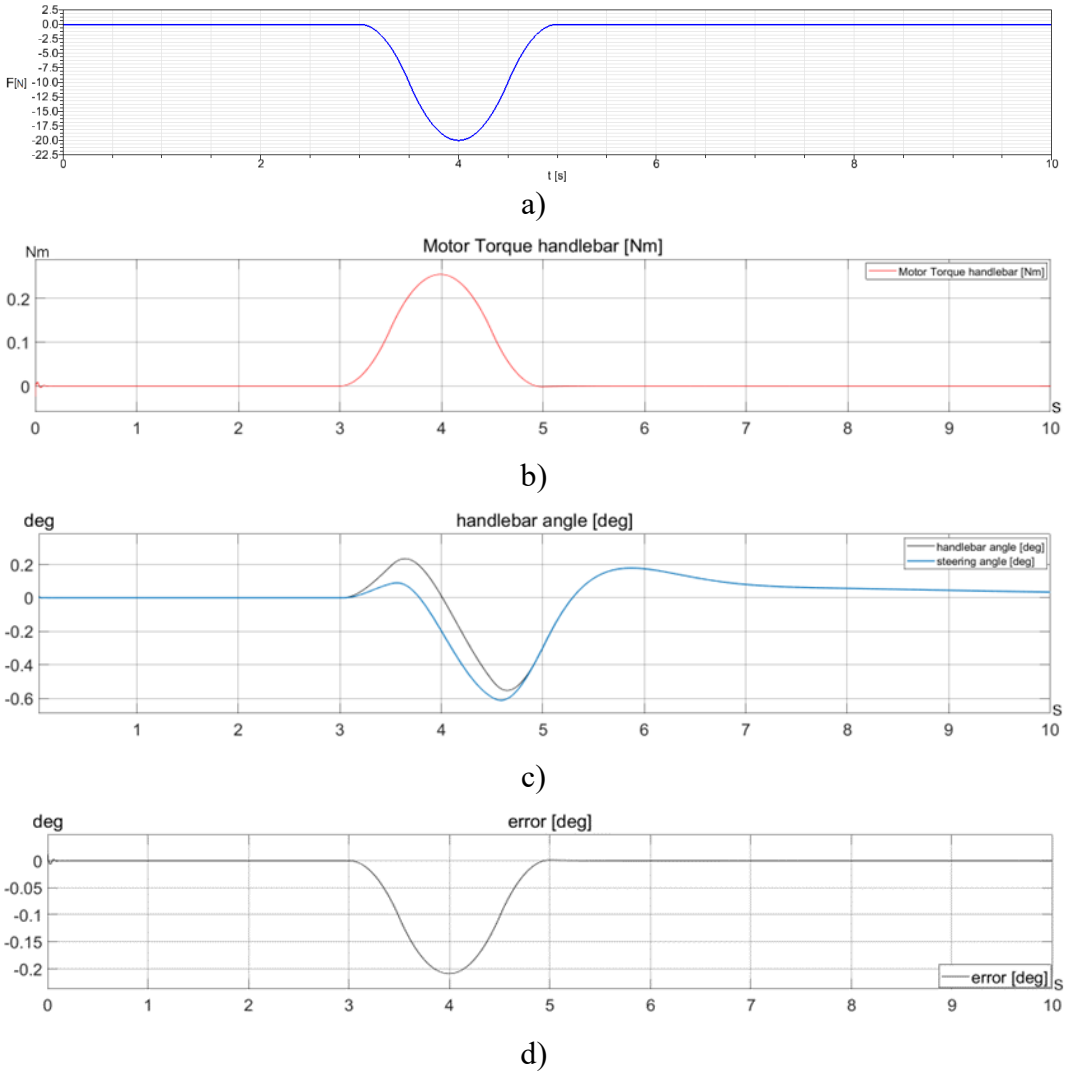

Figure 43: 10 seconds run with a 20 N force applied on the edge of the handlebar (a)). It is shown the b) response Torqe from the upper motor coming from the PD controller, c) the handlebar angle and steering angle overlayed and d) their error.

Looking at the reaction of the system to a 20 Nm force perturbation applied to the extremity of the handlebar while the bicycle was running at 4 m/s shows an excellent angle tracking and following despite a small delay in reaction time and an error rising to 0.2 degree, which can be considered as sufficiently low not to worry about. The torque the motor exerts to cope with the manoeuvre is sensibly low and then acceptable.

CONCLUSIONS

This research focused on how the implementation of a steer by wire system on a Powered Two-Wheelers (PTW) single track vehicle model could successfully lead to enhancing lateral stability and improving control characteristics especially at lower speeds, through a set of hardware-software features. Here, the problem of correcting the vehicle behaviour required an approach to a Multibody Simulation (MBS) software, Simpack, to build a reliable bicycle model to be used as real-dynamic tool to be connected to a numerical simulation environment containing the control law and architecture, Matlab-Simulink, through the method of the Co-Simulation. The first has been fundamental to set up and design the core mechanical hypothesis of the steer by wire bicycle, the physical disconnection between the handlebar and the rest of the fork, while the second served to build control strategies which can guarantee both lateral stability improvements and minimal change in rider perception.

The aim has been the developing of a stabilisation strategy based on the states of the bicycle and providing the additional torque to the lower motor and then interfacing the rider inputs with the handlebar. This has been achieved, leading to an effective interconnection between the two elements which are correcting and communicating their position, while tracking the respective steering. Moreover, the configuration of two setups guarantees the choice between a more effective, incisive, and fast correction influence and a less intrusive one, yet useful to help stabilizing at lower speeds, but with a narrower range of functioning. No matter what setup, it is shown how both have significantly extended the stable forward speed region, considering that is at lower velocities, supposedly in the range 1.5-6 m/s that the system must be the most fundamental. Furthermore, a set of both simple disturbances and more complex runs prove the reliability of the method in a wide range of speeds when facing external inputs which would put in difficult conditions an uncontrolled bicycle.

Finally, giving the rider the feeling of a traditional mechanical link is a challenge that has been addressed at the actual stage and carried out successfully using a PD controller on the handlebar; the system's behaviour can cope with the trial of

delivering accurate feedbacks to the driver as shown in the results. Nevertheless, more complex manoeuvres could be performed, implying steady cornering or slaloms could shed even more light on the human-bicycle interaction and perception.

Future improvements could concentrate on the optimization of the dynamics of the motors and the steer by wire elements, including magnetic field interactions with the motors, damping and stiffness of the belt driven connection and more precise estimations of the hardware masses. The actual model is a robust and trustworthy tool to assess the feasibility of the methods analysed and, after advancements, it will be a solid foundation for the implementation of such technology on a physical bicycle. This promises to lead to safer technological solutions, allowing improvements in two wheels mobility and advancing our understanding in human-bicycle interaction.

Bibliography

A. L. Schwab, N. A. (2013). Dynamics and Control of a Steer-by-Wire Bicycle. *Proceedings, Bicycle and Motorcycle Dynamics 2013*, (p. 7). Narashino, Japan.

Ernest P. Hanavan. Jr., C. U. (October, 1964). *A mathematical model of the human body.* USAF Institute of Technology.

Franklin, G. P. (1997). *Franklin, G.F., Powell, D.J., and Workman, M.L.* Prentice Hall: Ellis-Kagle Press.

G. Dialynas, R. H. (2018). Design and implementation of a steer-by-wire bicycle. *7th International Cycling Safety Conference* (p. 11). Barcelona, Spain: Delft University of Technology.

Georgios Dialynas, C. C. (2022). Rider control identification in cycling taking into account steering torque feedback and sensory delays. *International Journal of Vehicle Mechanics and Mobility*, 26.

Johannes Edelmann, Martin Haudum, Manfred Ploechl. (2015). Bicycle Rider Control Modelling for Path Tracking. (p. 6). IFAC-(International Federation of Automatic Control).

Levine, W. S. (2011). Control System Fundamentals. In W. S. Levine, *Control System Fundamentals.* College Park, Maryland, USA: CRC Press.

Pacejka, H. B. (2012). *Tire and Vehicle Dynamics.* Delft: Tire and Vehicle Dynamics.

S. Lovato, M. B. (2022). An Active Steering Assistant System. *Proceedings of the World Congress on Engineering 2022*, (p. 8). London.

Sharp, D. J. (October 2006). Single-Track Vehicle Modeling and Control. In D. J. Sharp, *IEEE Control Systems Magazine.*

Sharp, R. S. (2008). On the Stability and Control of the Bicycle. *School of Engineering, University of Surrey*.

Whipple, F. (1899). The stability of the motion of a bicycle. *The Quarterly Journal of Pure and Applied Mathematics, 30(120):312–348.*

Acknowledgments

First, a special thanks to Professor Pastorelli for having taken my side from even before the start of the thesis; your constant support and belief in what I was doing, considering the challenges of working remotely, have been precious and helped me in reaching this milestone. To Florian Klinger and Professor Manfred Plöchl from TU Wien; to the first for the indispensable supervision provided with expertise, insights, and encouragement and to the second for the chance you gave me in welcoming in this project. I am extremely grateful to you all for your dedication, time, and effort you invested for me.

To Mom and Dad, I owe everything I have achieved and who I am today to you. Your guidance and support shaped my journey, teaching me how to overcome life's obstacles. I look to you for inspiration whenever I face new challenges. I also want to thank Aunt, Grandma, and Grandpa watching over us, for their unwavering support through the ups and downs. Your encouragement guided me through every decision and led me to this moment.

To my lifelong friends, Ale, Andre, Edo, Fra, Gibo, Ire, and Matti, thank you for sharing every moment with me, from dark nights at Sir to moments of laughter and frustration. You've been my constant companions through the years, and I appreciate your understanding when my studies kept me away. I'm confident that our friendship will continue to thrive in the future, and the memories we've created will endure.

To everyone who shared the most beautiful and diverse years of my life, whether at Poli or elsewhere, thank you for being by my side and contributing to my personal growth. Special thanks to Viale Olimpia, which welcomed me into its home and say goodbye after months of unforgettable experiences that changed me. To those who uplifted me during difficult times through long conversations, and to those I couldn't mention, your contributions have made a lasting impact on my journey.

To my Vienna People. You shared with me one of the most incredible, variegated periods of my life. I cannot tell how much I learned from each one of you and how much I enjoyed this life experience. You got along with me in the final challenging stint of this long path, and I couldn’t wish for anybody else better for that. I wish you all to succeed in life in all the respective fields, you people are amazing.

And finally, to you, who never gave up, who knew how to rise again, who built a path for yourself that would have been unthinkable to tell at the beginning. Never stop trying to improve yourself. Always believe and don't be afraid to question yourself.

Never say never, because limits, like fears, are often just an illusion.